XXVII Manuel Rocha Lecture

Manuel Rocha (1913-1981) was honoured by the Portuguese Geotechnical Society with the establishment of the Lecture Series bearing his name in 1984.

Having completed the Civil Engineering Degree at the Technical University of Lisbon (1938) he did post-graduate training at MIT. He was the driving force behind the creation of the research team in Civil Engineering that would lead to the foundation of the National Laboratory for Civil Engineering (LNEC), in Lisbon. He was Head of LNEC from 1954 to 1974 and led it to the cutting edge of research in Civil Engineering.

His research work had great impact in the area of concrete dams and rock mechanics. He was the 1st President of the International Society for Rock Mechanics and organized its 1st Congress in Lisbon (1966). He did consultancy work in numerous countries. He was Honorary President of the Portuguese Geotechnical Society, having promoted with great commitment the cooperation between Portugal and Brazil in the area of Civil Engineering, and member of the National Academy of Sciences of the USA. Recognized as a brilliant researcher, scientist and professor, with a sharp, discerning intellect allied to a prodigious capacity for work and management, he was truly a man of many talents.

Prof. **L.I. González de Vallejo**, Emeritus Professor of Geological Engineering at Universidad Complutense de Madrid (UCM). PhD (UCM) and MSc (Imperial College). Director of the MSc Courses in Geological Engineering at UCM (1990-2008). He has dedicated his professional career in geological engineering to teaching, research and consulting, and he has conducted a large number of geological and geotechnical investigations in Spain and Central and South America. Has written 150 scientific papers and five books. Past-Chairman of the JTC3 on Education and Training of FedGIS. He has been invited to present the 2nd Ing. Mariano Ruiz Vazquez Memorial Lecture at the Academy of Engineering of Mexico (2007) and the 27th Manuel Rocha Lecture at the Portuguese Geotechnical Society and the Associação de Geotécnicos Antigos Alunos da UNL (2010).

Soils and Rocks
v. 35, n. 1

Design with Geo-Hazards: An Integrated Approach from Engineering Geological Methods

L.I. González de Vallejo

Abstract. An engineering geological approach to analysed geo-hazards affecting engineering and planning design decisions is presented. The methodological procedures include hazard identification, hazard assessment, site vulnerability, economic cost, environmental impact, risk assessment, social acceptability, decision analysis and engineering design criteria. The practical application of the Engineering Geological Methodology (EGM) is shown in several case studies: dam safety problems due to slope instability and induced seismicity during reservoir filling; seismic hazard assessment in regions with insufficient seismic data and tectonic information; and large scale geo-hazards due to giant landslides and related tsunamis. The EGM approach can provide fundamental criteria for engineering decisions and territorial planning. Social acceptability should be included in the decision analysis being evaluated according with the hazard level of the geological process and the corresponding risk of the affected elements. Examples of geo-hazards and their social acceptability are presented.

Keywords: geological hazards, engineering geology, hazard assessment, risk assessment, Canary Islands, Tenerife.

1. Introduction

One of the first books to include geological factors as a conditioning parameter of urban and infrastructure planning was Ian McHarg's pioneering "Design with Nature" published in 1969. Now, more than 40 years later, these criteria are well established and concern for the environment has grown to the point where it is one of the most critical factors in any large engineering project. However, it is only in recent times that natural hazards have been properly accounted for in engineering design and infrastructure planning. This concern is reflected in the title of this lecture: "Design with Geo-Hazards".

The approach presented here is based on engineering geological methods to provide solutions to the geo-hazards problems involved in engineering design decisions. Engineering Geology (EG) helps to reduce risk effectively, to design and build safer and more economical infrastructure, and to ensure environmental compatibility.

The term geological hazards -or geo-hazards- usually refers to earthquakes, landslides, volcanic eruptions or tsunami because of their catastrophic effects. However, there are also other minor damaging geo-hazards that have to be considered, such as those listed in Table 1. The effects of geo-hazards are usually accompanied by other related phenomena. Earthquakes can induce a variety of associated hazards such as ground shaking, surface deformation and faulting, liquefaction, landslides, rockfalls and tsunamis. Hydrometeorological hazards, such as floods or heavy rain, can also cause landslides, rockfalls, earth and debris flows on slopes. The nature of the geo-hazards and their consequences at a particular site should always be considered when a large engineering or land planning project is undertaken.

One of the main applications of EG, as the science applied to the study and solution of problems produced by the interaction of the geological environment and human activity, is the evaluation, prevention and mitigation of geological hazards. Problems arising from the interaction between human activities and the geological environment make appropriate actions to balance natural conditions and land use with geological hazard prevention and mitigation methods that are essential at the planning stage. These actions should have as their starting point an understanding of geodynamic active processes and of the geomechanical behaviour of the ground.

Damage related to specific geological processes depends on:

- The speed, magnitude and extent of the process.
- Whether actions can be taken to control the process or protect elements exposed to its effects.

The effects of ground movements may be direct or indirect, short or long term or permanent. Some tectonic or isostatic processes develop on a geological time scale, what means that their effects cannot be considered on a human scale. Only certain processes, when they occur on an engineering or geotechnical scale, can be controlled by human action, such as landslides or rockfalls, erosion, subsidence and floods. Others, such as earthquakes, tsunamis, volcanic eruptions and large scale landslides are outside the scope of human control. Here the importance of considering the influence of Earth dynamic processes on the design and safety of engineering works and installations. The follow-

L.I. González de Vallejo, Professor of Geological Engineering, Universidad Complutense de Madrid, Spain. E-mail: vallejo@geo.ucm.es.
Invited Lecture, No discussion.

Table 1 - Geological and meteorological processes which may cause risk (González de Vallejo & Ferrer, 2011).

Processes	Risk
External geo-dynamic processes	- Landslides and rock falls - Collapse and subsidence - Erosion - Expansivity and collapsibility of soils
Internal geo-dynamic processes	- Earthquakes and tsunami - Volcanic activity - Diapirism
Meteorological processes	- Torrential rain and intense precipitation - Flooding and flash floods - Gully erosion processes - Hurricanes - Tornados

ing sections present fundamental aspects related to the evaluation of geological hazards for engineering projects.

2. Hazard, Risk and Vulnerability

In hazard studies specific terminology is used to define hazard, risk and vulnerability. The term "hazard" refers to any more or less violent process which may affect people or property; it is often taken to be synonymous with "risk", although the two concepts are not the same. Hazard refers to the geological process, risk to the losses and vulnerability to damage. These concepts will be defined, according to how they are generally used.

Hazard, *H*, refers to the frequency with which a process occurs and its location. It is defined as the probability of occurrence of a potentially damaging phenomenon at a specified level of intensity or severity for a given time within a specific area (Varnes, 1984). To evaluate hazard, the following information is needed:

- Where and when the processes occurred in the past.
- Their intensity and magnitude.
- The areas where future processes may occur.
- The frequency of the occurrence.

This last point can only be estimated if the process timeframe is know (*e.g.* the return period for earthquakes or floods, from historical or instrumental data series), or for the triggering factors (*e.g.* the return period for rainfall that triggers landslides in a certain area).

Hazards, as it has been explained, can be defined as the probability of occurrence of a phenomenon of specific intensity within a given period, but can also be expressed using the return period *T* (years elapsing between two events or processes of similar characteristics), which is the inverse of the annual exceedance probability, *P*(*a*):

$$T = 1/P(a) \quad (1)$$

The probability *p* that a specific intensity value (*e.g.* an acceleration value in the case of earthquakes) corresponding to an average return period *T* (years) will be exceeded during a specific time period *t* is expressed as:

$$p = 1 - \left(1 - \frac{1}{T}\right)^t \quad (2)$$

The time *t* (years) can be the service life of a dam or building, that is, the expected exposure time or useful life of the structure. Table 2 shows the service life of different installations; Fig. 1 gives the probability of exceedance curves as a function of this parameter and of the return period *T*.

The concept of risk, *R*, includes socio-economic considerations and is defined as the potential losses due to a specific natural phenomenon (human lives, direct and indirect economic losses, damage to buildings or structures, etc.). At the present time, the risk of earthquakes is the most widely developed. Seismic risk is defined as the expected losses that structures will suffer during the period they are exposed to seismic activity; this time period is known as the exposure time or service life of the structure, as has been mentioned above.

Risk is evaluated starting from the hazard corresponding to a particular process (cause) and the effects of this on the elements exposed to the hazard (consequences). These effects on the exposed elements (buildings, infrastructures, people, etc.) may be expressed by different pa-

Table 2 - Service life of different installations (*t*) (González de Vallejo & Ferrer, 2011).

Structure or installation	*t* (years)
Storage of radioactive waste	10,000
Nuclear power stations	40-80
Dams	100-150
Bridges, tunnels and major infrastructure works	100
Storage of toxic waste	250
Conventional buildings and structures	50-70

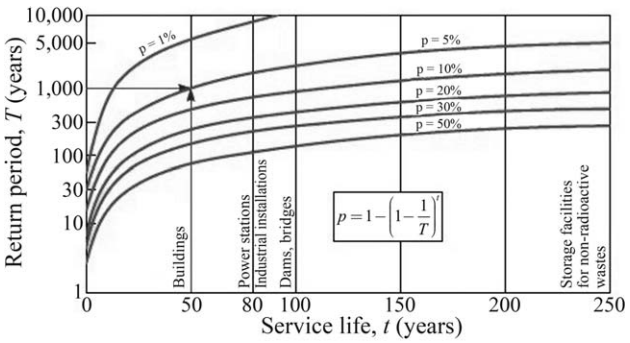

Figure 1 - Probability of exceedence (*p*) of an event of known return period occurring in the service life of a structure (González de Vallejo & Ferrer, 2011).

rameters: vulnerability, losses, cost, exposure, etc. The risk and the hazard refer to a specified time period, and may be evaluated in either deterministic or probabilistic terms.

The risk can be calculated from the expression:

$$R = H \text{ x } V \text{ x } C \quad (3)$$

where H is the hazard of the process in question, V is the vulnerability of the elements exposed to the process (elements at risk) and C is the cost or value of these elements. As described above, the risk is expressed in losses (human or economic); in the expression above, these "unit" correspond to C, while H is a probability and V an adimensional parameter, as is explained below. The value of C can be expressed in either deterministic or probabilistic terms; if the latter, the risk will also be obtained in terms of probability.

If any of the factors is zero, the risk will be zero; this means that in a high hazard zone, the risk will be zero if there are no element exposed, or if the vulnerability of these is nil. People may increase the risk by occupying hazardous zones, affecting the intensity of the processes or triggering them and by constructing vulnerable buildings or structures. The risk can be reduced by reducing the hazard (acting on the process control factors where this is possible) or the vulnerability (acting on the elements exposed to the risk).

According to Smith (2001) risk can be defined as the probability that a hazard will occur and cause losses, and is evaluated from the expression:

$$R = P \text{ x } Le \quad (4)$$

where P is the occurrence probability of the process, or hazard, and Le the expected losses.

The product H x V is known as specific risk and is defined as the level of losses expected during a given time period resulting from the occurrence of a specific process, expressed in terms of probability. In this case, a quantitative evaluation of losses cannot be made (Varnes, 1984). According to the UNESCO definitions, the risk can be evaluated as follows:

$$R = H \text{ x } V \text{ x } E \quad (5)$$

where E is the exposure of the elements at risk. Because of the difficulty of quantifying the variable E and considering that for some authors exposure is included in vulnerability (an element is not vulnerable if it is not exposed to risk), the expressions above are more appropriate, when the cost of either the exposed elements, C, or the expected losses, Le, are considered directly for a specific occurrence.

Vulnerability, V, is the expected degree of damage or loss in an element or group of elements at risk resulting from the occurrence of a hazard of specific intensity or magnitude. It depends on the characteristics of the element considered (not on its economic value) and on the intensity of the phenomenon; it is usually evaluated on a scale from 0 (no damage) to 1 (total loss or destruction of the element) and from 0 to 100% damage.

In the case of seismic risk, the vulnerability of a structure or group of structures, or of whole urban area, is defined as its intrinsic predisposition to sustain damage if a seismic movement of a specific intensity occurs. This will depend on the structural design characteristic and on the intensity of the earthquake; it means that the vulnerability of a masonry building is higher than that of a concrete building during an earthquake. This parameter is usually defined through vulnerability functions that can be established from the damage or losses such processes have caused in the past and/or from the hypothetical potential damage these phenomena would cause were they to occur. In both cases, present-day measures to reduce or mitigate the potential damage have to be taken into account, as these reduce the vulnerability of the exposed elements.

3. Geological Engineering and Engineering Decisions

In geological engineering it is normal practice to estimate safety criteria by using a factor of safety FS, as a deterministic indicator of the relationship between the stabilizing and destabilizing forces (in a limit equilibrium situation $FS = 1.00$). The factor of safety can be defined as the coefficient by which the ground shear strength must be reduced for a slope, excavation, foundation, etc. to reach a state of limit equilibrium (Morgenstern, 1991). The value chosen for this factor depends on how much is known about the ground strength parameters, hydrostatic pressures, potential shear surfaces and the magnitude of the external forces which act or may act on the ground (Hoek, 1991).

A satisfactory solution to the geological and geotechnical problems which may arise from interactions between the ground and the structures depends on the correct selection of geomechanical parameters, the application of the appropriate analytical tools and the choice of reasonable safety and acceptability criteria. Table 3 shows some acceptability criteria for different types of structures.

When geological processes may occur with potentially damaging results, these processes must be considered in the stability and safety of the project. Once the process has been identified (earthquake, flood, landslide, etc.) and the level of severity has been defined using parameters such as seismic acceleration, water height and speed, these parameters are integrated into the factor of safety calculation.

There are standards or regulations which specify the factor of safety, return period and other criteria that must be used depending on the project type and function. If there are no codes or specific safety requirements, the decision is usually left to the expert judgement or criteria of the designer. The following factors of safety are given as guidelines:

- For ground failure conditions:
  - Short-term engineering works with no structures involved (opencast mining, temporary slopes, etc. which do not form a supporting part of foundations or structures): $1.2 \leq FS < 1.5$.

  - Long-term engineering works with no structures involved: $FS \geq 1.5$.
  - Foundations and excavations involving structures: $1.5 \leq FS \leq 3.0$.
- The effects of a particular event that may affect an engineering structure due to a geo-hazard is usually related to the return period T of such an event. The following T values are suggested:
  - Conventional buildings and structures: $100 \leq T \leq 500$ years.
  - Major structures, dams, bridges, significant buildings: $T = 1{,}000$ years.
  - Critical facilities: $1{,}000 \leq T \leq 10{,}000$ years or the equivalent of the recorded maximum historical intensity level.

When a geological process causing a potential hazard has been identified in terms of intensity and return period, then the probability p of this hazard being exceeded during the service life of the structure is calculated, using the following criteria:

- Major structures: $p \leq 10\%$
- Critical facilities: $p \leq 5\%$.

Excluded from these criteria are some exceptional geological phenomena with extremely low probability, *e.g.* major tsunami, large landslides or maximum potential earthquakes according to geological data.

4. Geo-Hazard Assessment by Engineering Geological Methods

Engineering geology and geotechnical engineering are related terms that integrate knowledge from geological and engineering sciences and technologies with engineering and the environment in a wide range of activities. When a project has to be implemented in a particular region exposed to natural hazards, the engineering design has to consider a variety of concepts using the criteria needed to ensure safe and economical solutions.

Managing geological, statistical, social and engineering data is a complex task due to the different criteria, time and spatial scales used. Geological Engineering (GE) can provide a link between geo-scientific information and engineering requirements. This is possible because GE uses a language common to both engineers and geo-scientists and is based on a common geological and engineering background. A procedure based on practical experience that integrates geological and geo-engineering methods is described below to provide specific answers for engineering solutions when geo-hazards have to be considered. The procedure includes the following points:

1. Hazard identification: intensity, size and scale of the phenomenon.
2. Hazard assessment: frequency, probability and maximum potential event.
3. Site vulnerability evaluation.
4. Economic cost estimation.
5. Environmental impact assessment.
6. Risk assessment.
7. Social acceptability evaluation.
8. Decision analysis.
9. Engineering design criteria

Hazard assessment is usually carried out by deterministic and probabilistic methods. Deterministic methods conventionally adopt the maximum historical or characteristic event, which usually leads to a very conservative result. However, these methods do not provide the uncer-

Table 3 - Acceptability criteria in relation to different types of engineering structures and excavations (modified from Hoek, 1991).

Engineering structures	Acceptability criteria
Soil slopes	$FS > 1.3$ for "temporary" slopes. $FS > 1.5$ for "permanent" slopes.
Rock slopes	$FS > 1.3$ for "temporary" slopes. $FS > 1.5$ with probability of failure of 10 to 15% may be acceptable for open pit mine slopes.
Earth dams	$FS > 1.5$ for full pool. $FS > 1.2$ for probable maximum flood with steady state seepage and > 1.0 for full pool with steady state seepage and maximum credible horizontal pseudostatic seismic loading.
Gravity dams	FS against foundation failure > 1.5 for normal full pool operating conditions. $FS > 1.3$ for probable maximum flood. $FS > 1$ for extreme loading-maximum credible earthquake.
Arch dams	FS against foundation failure > 1.5 for normal full pool operating conditions. $FS > 1.3$ for probable maximum flood.
Foundations	Bearing capacity failure should not be permitted for normal loading conditions. Differential settlement should be within limits specified by structural engineers.
Rock tunnels	FS including the effects of reinforcement, should exceed 1.5 for sliding and 2.0 for falling wedges and blocks.

tainty or reliability of the characteristic event. Uncertainty evaluation is a high priority issue and also one of the main problems when dealing with geo-hazards.

Probabilistic methods can provide a quantitative value for uncertainties and there are different procedures available for probabilistic analysis. The Cornell method (Cornell, 1968) is widely used for probabilistic seismic hazard assessment (PSHA). An example of the application of this method is shown in Section 6.6. Other examples of PSHA applied to critical facilities in Spain are described by González de Vallejo (1994), and an example of its application to active fault hazard assessment for a dam in Portugal is given by Gomes Coelho (2005).

Logic tree methods can be a useful tool for hazard analysis quantification, giving a number of possible consequences resulting from an initial event. The sequence of subsequent events needs to be identified and the probability of occurrence quantified. An example of logic trees applied to uncertainty evaluation in slope stability analysis is shown in Fig. 26, Section 7.4 of this paper. Whitman (1984) presents several applications of this methodology and Bommer *et al.* (2005) apply logic trees to seismic hazard analysis.

The Monte Carlo simulation method is another useful probabilistic procedure for geo-hazard analysis. This simulates stochastic processes by repeated random sampling of inputs to an analysis model in proportion to their joint probability density function. A description and example applications of Monte Carlo simulation are shown in Nadim (2007). A comprehensive review of probabilistic methods for risk assessment and geotechnical applications is given by Fenton & Griffiths (2008).

Probabilistic and deterministic methods are both necessary for geo-hazard analysis. However, each of them has advantages and disadvantages as shown in Table 4. Although probabilistic methods are currently the most used, they are not a substitute for deterministic methods but are complementary to them (CETS, 1995).

The results of the hazard assessment can be used to evaluate site vulnerability of exposed elements, the economic and environmental consequences if failure occurs and for risk assessment.

Social acceptability can be expressed as the level of acceptance of risk from hazards which may cause loss of life and material or environmental damage in the short, medium or long term. Social acceptability is a subjective concept that depends on many different factors, including regional or country acceptability of risk in a particular project or facility. It can also be considerably affected if disasters occur such as dam failure or a nuclear power plant accident.

Given that social acceptance or rejection of the risks from natural hazards depends on multiple variables which may change over time in different circumstances, the level of social acceptability has to be quantified depending on parameters related to the hazard (probability) and their consequences. For example, the following descriptors for dam failure probability (p_f) are used by the U.S. Bureau of Reclamation:

- Virtually certain	$p_f = 0.999$	Unlikely	$p_f = 0.1$
- Very likely	$p_f = 0.99$	Very unlikely	$p_f = 0.01$
- Likely	$p_f = 0.9$	Virtually impossible	$p_f = 0.001$
- Neutral	$p_f = 0.5$		

These probability values do not include failure due to the effects of geo-hazards with probabilities lower than 10^{-3}.

Whitman (1984) used annual probability of failure versus both costs and number of fatalities for a wide variety of project types, with the annual probability of failure of commercial aircraft around or lower than 10^{-6}. Because people generally accept this type of transport as acceptable and safe, this threshold value can be considered as an acceptable risk by society.

On the other hand, in some European countries the probability of occurrence of a particular geo-hazard during the service life of the structure can be ranked in the following intervals:

Table 4 - Some experts' opinions on using deterministic and probabilistic methods for seismic hazard assessment (modified from González de Vallejo, 1994).

	Deterministic	Probabilistic
Advantages	Appropriate if one has complete knowledge of the seismogenetic models. Recommendable for areas with high seismicity. Recommendable for top security installations.	Suitable for areas with low and moderate seismicity. The uncertainties can be incorporated and dealt with. The frequency of earthquakes can be dealt with.
Disadvan-tages	It requires good geological data. It may give unacceptable results from an economic point of view, it may be equivalent to a probability of 10^{-4}-10^{-5}. It does not take the uncertainties into account. In "stable" regions the uncertainties may be so great that it should not be applied. The inclusion of new data (*e.g.*: paleoseismicity) may substantially modify the result.	The Poisson model is not suitable either for major earthquakes or for the Gutenberg and Richter distribution. Prediction of earthquake magnitudes greater than 5.0 cannot be made by probabilistic methods with an accuracy that is meaningful for site specific evaluations in engineering.

- Low probability: $10^{-2} > p \geq 10^{-3}$
- Very low probability: $10^{-3} > p > 10^{-4}$
- Extremely low probability: $p < 10^{-5}$
- Remote probability: $p < 10^{-6}$

Therefore those geo-hazards with an occurrence probability lower than 10^{-4} can be considered as acceptable in terms of risk according to some codes and regulations. But acceptability is also highly dependent on the consequences of failure. This is the case of nuclear power plants or radioactive waste repositories that require a geo-hazard occurrence probability much lower than 10^{-6}. Although social acceptability is a difficult question to estimate, it is an increasingly important issue that should be considered and integrated into the decision analysis procedures when dealing with geo-hazards risk assessment.

Social acceptability criteria can be related to hazard, vulnerability and risk. Table 5 presents an example of acceptability criteria assessment for different types of infrastructures. Geo-hazard probability and vulnerability are related with the degree of losses, *e.g.* economic costs and fatalities, and environmental impacts. Risk is classified in 3 categories: I (acceptable), II (acceptable with restrictions) and III (unacceptable). Restrictions mean that the engineering solutions have to be improved to reach an acceptable level of risk, either by selecting an alternative site with lower level of hazard or by decreasing the vulnerability by engineering design solutions, or both.

Decision analysis is a necessary exercise for the analysis of the information described above. At this stage, logic tree methods are useful tools for integrating data to help decision-making. After this analysis process, design criteria have to be based on safety requirements, cost optimization and environmentally compatible solutions. A compromise solution between cost and safety should be agreed, keeping in mind that increased safety means exponentially increasing costs.

The following sections present three case studies of practical applications of engineering geological methods to engineering and territorial planning with different types of geo-hazards.

5. Landslide and Seismic Hazards in Dam Safety: The Itoiz Dam Case Study

The Itoiz dam was designed with the opposition of the people living downstream who had been alerted by technical reports to the unsafe conditions of the dam due to landslide instability of the left slope of the reservoir close to the dam site. During the first reservoir filling, a series of earthquakes were felt near the dam and public opposition led to legal action demanding closure of the dam. An independent Commission was set up to report on the potential geological hazards affecting the dam safety (González de Vallejo *et al.*, 2005). New investigations were also carried out (González de Vallejo *et al.*, 2009). This gravity type dam (height: 122 m, length: 525 m, reservoir: 418 Hm^3) is for irrigation and water supply and has been in operation since 2008. The dam is 22 km eastern of Pamplona, northern Spain (Fig. 2).

Figure 2 - Itoiz dam and reservoir, located 22 km east of Pamplona, northern Spain.

Table 5 - Social acceptability criteria in relation to hazard, vulnerability and risk.

Hazard probability p_f	Vulnerability: losses and environmental impacts in case of failure											
	Conventional structures				Large infrastructures				Critical facilities			
	L ST	M ST	H MT	VH MT	L ST	M MT	H MT	VH LT	L ST	M MT	H LT	VH LT
$\leq 10^{-2}$												
$\leq 10^{-3}$									III			
$\leq 10^{-4}$			II									
$\leq 10^{-5}$				I								
$\leq 10^{-6}$												

p_f = Annual probability of failure.
Risk: I = Acceptable, II = Acceptable with restrictions, III = Unacceptable.
Losses: L = Low, M = Medium, H = High, VH = Very high.
Environmental impacts: ST = Short term, MT = Medium term, LT = Long term.

5.1. Engineering geological investigations

The main aim of the investigation carried out was to determine the slope stability conditions regarding possible earthquakes and precipitation for 500, 1,000 and 5,000 year return periods. The methodology used required the following investigations:

- Neotectonics and fault activity:
  - Identification and characterization of the seismogenetic faults in the area.
  - Absolute dating of the Quaternary deposits affected by recent tectonic deformation.
  - Relationship between faults and seismicity.
- Seismic hazard:
  - Compilation of a joint Franco-Spanish unified seismic catalogue.
  - Characterization of possible seismogenetic sources depending on seismic and tectonic information.
  - Probabilistic seismic hazard analysis for 500, 1,000 and 5,000 years return periods in terms of the horizontal peak ground acceleration (PGA).
  - Uniform hazard response spectra and compatible earthquake accelerograms.
- Hydrological and hydrogeological surveys:
  - Pluviometry, temperature and climate classification.
  - Surface run-off and water balance.
  - Groundwater flow models.
- Geological and geomechanical description:
  - Geological-geotechnical mapping.
  - Boreholes, in-situ tests, geophysical surveys and laboratory tests.
  - Evolution and absolute dating of landslides.
  - Hydrogeological characterization of materials.
  - Geotechnical classification of materials and their strength and deformational properties.
- Slope stability analysis:
  - Geological, hydrogeological and geomechanical models.
  - Stability analysis using limit equilibrium and stress-strain methods
  - Critical landslide surfaces, safety factors, maximum displacement and deformation for different hypotheses.
  - Influence on slope stability of strength properties, piezometric levels and seismicity.
- Slope instrumentation and monitoring:
  - Installation of piezometers, inclinometers, extensometers and surface movement control points.
  - Analysis and relationships between piezometers and inclinometers and surface movements.

5.2. Tectonic and seismicity studies

5.2.1. Fault activity

The results of the surveys carried out in the area within a 25 km radius of the Itoiz dam identified 3 faults with possible seismic potential. No morphological expressions were found in the area which display quaternary activity in the faults. The maximum potential seismicity associated with these faults has been estimated at around $M = 6.5$ for a return period of over 6,000 years. The results of thermoluminescence dating show that the tectonic deformations associated with the faults are less than 125,000 years old, *i.e.* Upper Pleistocene.

5.2.2. Seismicity during the first reservoir filling

A large number of low magnitude earthquakes were recorded near the dam site during the first reservoir filling (2004), the largest of magnitude 4.6. (Figs. 3 and 4). Table 6 shows a summary of the criteria used following Simpson (1986), Gupta (2002) and McGarr *et al.* (2002), which show that the type of seismicity recorded in the area surrounding the dam responds to the concept of triggered seismicity, not induced seismicity (Boomer *et al.*, 2005). The earthquake triggering due to the reservoir filling would be what could occur in the future from natural, not induced causes. The maximum earthquake corresponding to this type of triggered seismicity could be associated with the normal faults present in the area with potential magnitude lower than 5.5 for 1,000 year return period.

5.2.3. Seismic hazard

The seismic actions of earthquakes corresponding to 500, 1,000 and 5,000 years return periods were characterized from the seismic hazard curve obtained for the dam site, expressed as the PGA. The PGA value obtained for a 500 year return period was 0.08 *g*; for a 1,000 years return

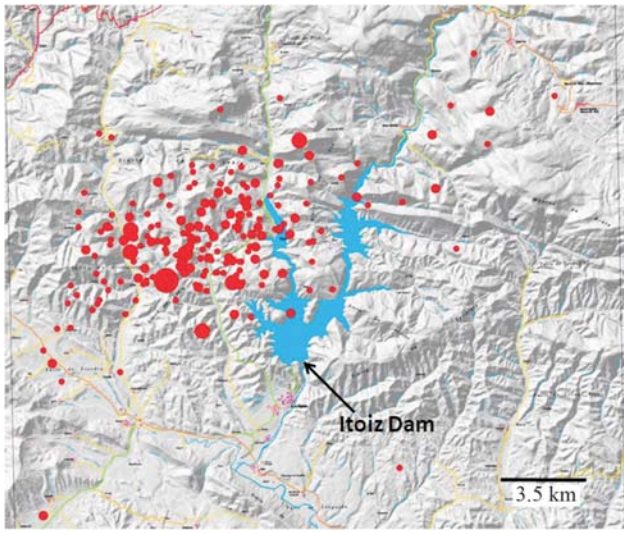

Figure 3 - Epicentres of earthquakes recorded during the first reservoir filling.

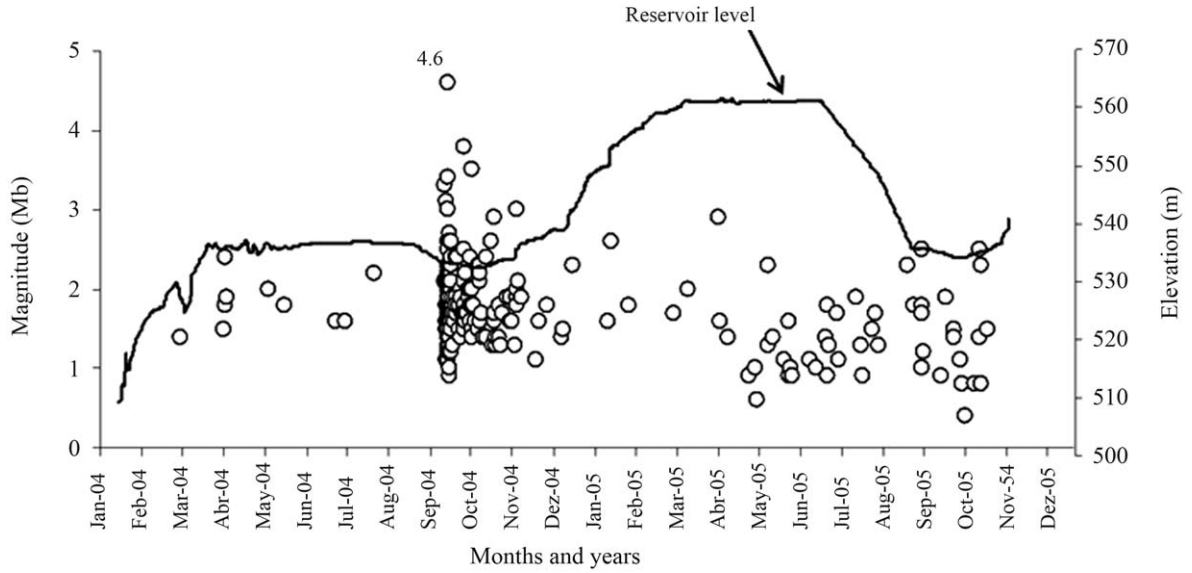

Figure 4 - Earthquake magnitudes during the first reservoir filling.

Table 6 - Triggering seismicity criteria in Itoiz dam (González de Vallejo *et al.*, 2005).

Triggering criteria	Itoiz dam				Triggering seismicity	
					Yes	No
Coincidence in time (< several years)	9 months after initiation reservoir filling; 5 months after reached maximum elevation				X	
Spatial distribution						
Epicentres (< 20 km)	4-7 km				X	
Hypocentres (< 30 km)	3-8 km				X	
Reservoir located in low/moderate seismic zone	Moderate / Low seismicity				X	
Normal or strike-slip faults	Normal faults				X	
Seismic parameters						
Parameter *b*:						
$b_{pre} > b_{after}$	$b_{pre} = 0.42$ $b_{after} = 1.12$					X
$b_{trig} > b_{nat}$	Itoiz	$b_{pre} = 0.42$ $b_{after} = 1.12$	*Nat*	$b_{pre} = ?$ $b_{after} = ?$	-	-
$b_{trig} > b_{rec}$	Itoiz	$b_{pre} = 0.42$ $b_{after} = 1.12$	$b_{reg} = 0.62$		-	-
Magnitude relationships						
M_{max}/M_0 (near 1)	$M_{max} = 3.8\ m_bLg$	$M_{max}/M_0 = 0.82$			X	
M_0 - M_{max} low (< 1)	$M_0 = 4.6\ m_bLg$	M_0 - $M_{max} = 0.8$			X	
Low decrease of the number of aftershocks with time ($h = 1$)	Itoiz	$h = 0.67$	*Nat*	$h = ?$	X	-
Mogi (1963) model distribution of aftershocks and premonitory seismicity	Type II				X	

b - Gutenberg-Richter parameter (see Table 10). *Nat* = "natural" seismicity to differenciate with "triggering" seismicity. M_0 = the largest magnitude event. M_{max} = the maximum magnitude of the aftershocks events. *h* = rate decrease of the number of aftershocks with time.

period it was 0.13 *g*; and for a 5,000 year return period it was 0.30 *g*. These PGA values are considerably higher than those calculated in the construction project for the dam and than those recommended in the Spanish earthquake resistant building standards (NCSE-02).

The most probable earthquake for a 1,000 years return period could reach a moment magnitude (M_w) of between 4.7 and 5.1, according to the possible seismogenetic sources and would take place in the immediate area of the dam (epicentral distance ≤ 5 km). For a 5,000 year return period the earthquake could reach a moment magnitude (M_w) of between 6.4 and 6.6, and would take place at an epicentral distance of 15-20 km.

5.3. Landslides stability analysis

The left slope of the dam is composed of the following materials (Figs. 5 and 6):

- Colluvial. Most superficial level, composed of gravel and cobbles in a sand-silt matrix with clays of up to 12 m thick. Presents high electrical resistivity values and low seismic wave propagation velocity. Highly permeable.
- Upper calcareous breccia (UCB). Composed of boulders and sub-angular gravel, with heterometric calcareous material contained in a low consistency sand-clay matrix. The matrix content is 45%. Presents areas with karstification. Very varied thickness, of up to 31 m. The permeability of these materials is very high.
- Lower calcareous breccia (LCB). This is composed of the same materials as the UCB. The matrix content is 55%. Variable thickness of up to 28 m. Presents slickenside surfaces. Higher seismic wave propagation velocity and lower electrical resistivity than the UCB. High permeability.
- Bedrock. Formed by stratified marls, limestones and calcarenites with 20°-25° dip. This is slighly weathered medium quality rock (Class III). High seismic wave velocity and electrical resistivity.

Figure 6 - Borehole cores of the calcareous breccias of the slided material.

The geomechanical properties of these materials are summarized in Table 7. The UCB and LCB deposits both correspond to landslide materials. Figure 7 shows their extension and situation in relation to the dam. The landslides occurred along stratification planes in the bedrock, with 20° -25° dip in the direction of the slope. The slickenside surfaces of the LCB layer correspond to failure planes.

Three landslides were identified on the left slope (L1, L2 and L3) which correspond to different episodes of successive landslides (Figs. 5 and 7). Their total volume is of the order of 3 x 10^6 m^3.

Figure 8 shows a detail of the slip materials observed in a trench (Gutierrez *et al.*, 2007). The absolute dating gives an age of 12 ka for the most recent landslide and 38 ka for the oldest one. These results indicate different reactiva-

Table 7 - Geomechanical mean properties of the materials of the left slope of Itoiz dam.

Material	Cohesion (kPa)	Angle of internal friction (°)	Young modulus (GPa)
Colluvial	10	30	2.6
UCB	50	32	5.0
LCB	70	30	6.6
Bedrock	-	-	25.2

UCB: Upper calcareous breccia. LCB: Lower calcareous breccia.

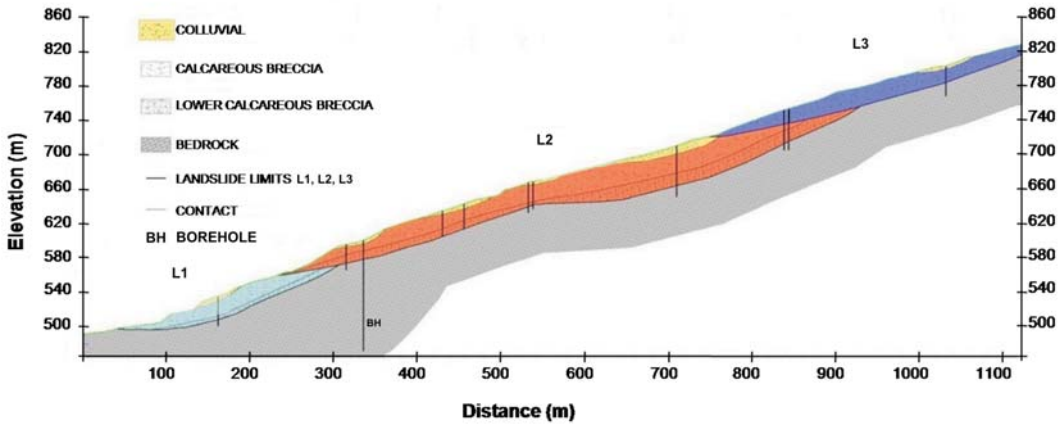

Figure 5 - Geological profile of the left slope of the reservoir near the dam site. L1, L2 and L3 correspond to 3 different landslides.

Figure 7 - Paleo-landslides area near the Itoiz dam.

tion periods of these movements, although no movements more recent than 12 ka were observed.

The failure surface strength, the slope saturation degree and the seismicity were evaluated. With regard to the strength properties of the materials, in particular the lower breccia (LCB), the values taken were $c = 70 \pm 50$ kPa and $\phi = 30 \pm 5°$, from the results of the laboratory tests. Different slope saturation degrees were assumed equivalent to a 23% saturation degree and to a 46% saturation degree, according to the hydrogeological data. However, full saturated slope hypothesis was also considered.

Different PGA values and accelerograms were considered depending on whether a pseudostatic or dynamic analysis, respectively, was applied. Slope stability was analysed using limit equilibrium and stress-strain methods for different scenarios. The results obtained are shown in Table 8 and in Figs. 9 and 10.

5.4. Slope instrumentation and monitoring

The left slope has been instrumented for over 10 years with numerous piezometers, inclinometers, extensometers and surface measurements with GPS. Most of the piezometers installed on the slope are dry and are not affected by the variations in the reservoir level or by the rainy periods in the area. Only the piezometers nearest the dam reproduce the variations in it. These results reflect the high permeability of the medium, its high hydraulic transmissivity and transversal drainage.

The manual inclinometers display extremely low displacements, which are mostly negligible or are within instrumental error limits. The greatest displacement, 17 mm, was obtained in an inclinometer near the dam. In the other inclinometers the maximum displacements were lower than 11 mm. The displacements recorded by the automatic inclinometers were very low, below the instrumental error limit.

The measurements taken on the surface with GPS show displacements lower than 15 mm. The results ob-

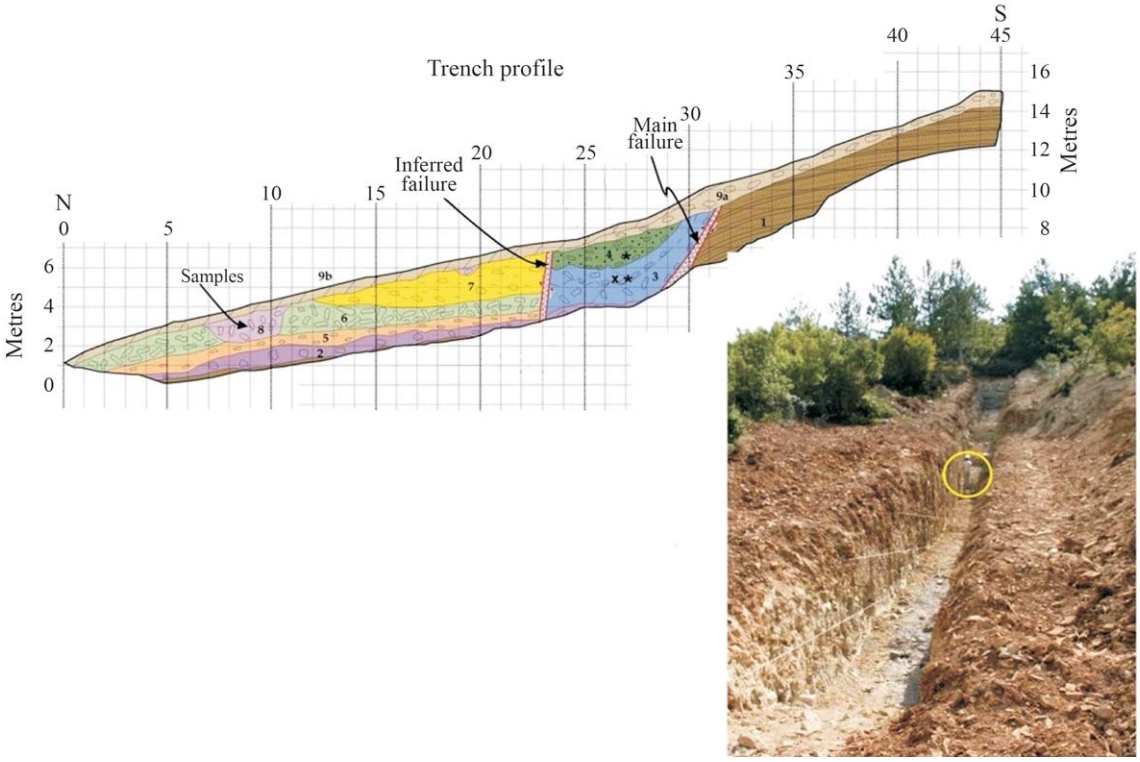

Figure 8 - Geological profile along a trench were detail sedimentological, geomorphological and geotechnical observations were carried out (modified from Gutierrez *et al.*, 2007).

Table 8 - Stability analysis results for the left slope of Itoiz dam.

Hazard scenarios	Design condition for 500 years RP	Design condition for 1,000 years RP	Extreme conditions for 5,000 years RP
DS (%)	5	23	46
PGA (*g*)	0.08	0.13	0.30
FS calculated	> 1.6	> 1.5	> 1.15
FS required by dam codes	> 1.3	> 1.15	> 1.0

DS: degree of saturation of the slope materials. RP: return period. PGA: peak ground acceleration.

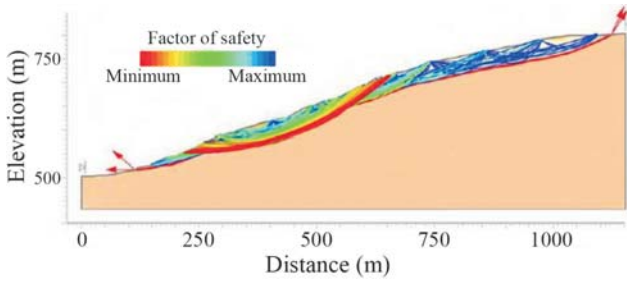

Figure 9 - Slope stability analysis by limit equilibrium methods showing critical failure surfaces for PGA = 0.13 *g*.

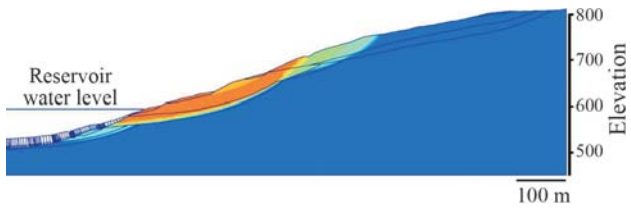

Figure 10 - Slope stability analysis by stress-strain analysis showing maximum displacements.

tained do not reflect any existing trend in the movements, since the displacements are erratic and do not occur in the same direction. An automatic topographical control system has been installed on the slope, which triggers alarms at different levels if the displacement thresholds established are exceeded. Since the system was installed no displacements higher than the instrumental errors have been recorded. The numerous monitoring systems installed on the slope have not detected movements of the ground or high piezometric levels.

5.5. Conclusions

The seismicity recorded during the first reservoir filling corresponds to the concept of triggered seismicity. That means that the reservoir filling itself will not generate seismicity, but it anticipates a natural seismic phenomena. The reservoir filling will not affect the seismic potential of the area, nor will it induce an earthquake higher than those considered or expected from slope and dam stability analysis.

The results obtained demonstrate that the left slope is currently stable, and also that it will continue to be stable even in extreme seismic and hydrogeological conditions.

6. Seismic Hazard Assessment in Regions with Insufficient Information: The Canary Islands Case Study

6.1. Introduction

Insufficient or incomplete seismic data can lead to great uncertainties and unreliable seismic hazard results even when the tectonic sources are unknown or not well identified. In many regions of the world the instrumental period of seismic records is too short and the historical seismic catalogue is incomplete. This is the case of the Canary Islands.

Few investigations have been carried out so far on seismicity and none on seismic hazard in this region. The Spanish Seismic Code (NCSE-02) is currently the only reference related to seismic hazard in the Canarian archipelago. This Code provides an updated version of the 1994 seismic-hazard map of Spain (NCSE-94). Both maps were derived in terms of macroseismic intensity, and then converted to a characteristic ground acceleration, which in practice is taken as peak ground acceleration (PGA), related to a 500 years return period. However, the probabilistic assessment was not performed for the Canary Islands either in the 1994 nor the 2002 version, and a 0.04 *g* PGA was arbitrarily adopted for the whole archipelago.

Conducting a seismic-hazard analysis of the Canarian Archipelago is plagued by important shortcomings. Very few tectonic structures have been described so far and seismic instrumental recording dates only since 1975. Historical seismic catalogue dates from the 14th Century and only the largest earthquakes have been recorded, including earthquakes with intensities of VIII and X, all related with volcanic eruptions. Nevertheless, assessing the seismic hazard is currently of prime importance for the near-future development of industrial facilities and urban expansion on the islands.

Tenerife, the most populated island, holds a density of population 5 times of Spain and 4 times of Europe. Even

low magnitude earthquakes can cause a great social alarm and seismic resistant design is not required in practice for building construction.

6.2. Geological and tectonic setting

The Canary Islands form a volcanic archipelago located on the passive margin of the African plate, 100 km off west Africa. Active volcanism has taken place on the islands in historical times, commonly together with the occurrence of volcanic-related seismic sequences, some of them felt as high as I_{MSK} = X. In the past 500 years several volcanic eruptions have taken place in Tenerife, La Palma, Lanzarote and El Hierro. The last eruptions occurred in 1971 on La Palma (Teneguía volcano). A new submarine eruption occurred in 2011 near the south coast of El Hierro.

Very few tectonovolvanic structures have been described yet in the Canarian Archipelago (Fig. 11). One of the first structures described were triple rift junction located in relation to the main volcanic centres on Tenerife and El Hierro (Navarro, 1974). Seismic exploration and marine geophysics have revealed the different crustal structure of the eastern islands to the western islands (Banda *et al.*, 1981; Carbó *et al.*, 2003). The eastern islands lie on a crust 15 km thick and form a very conspicuous north-northeast-south-southwest structure, the so-called East Canary Ridge. In contrast, the crust in the western islands is 11 km thick and structures show a general north-south trend.

The most important seismo-tectonic feature known in the archipelago is located between the islands of Tenerife and Gran Canaria (Fig. 12). In this area, a northeast-southwest-trending fault was first described by Bosshard & McFarlane (1970), and later, Mezcua *et al.* (1992).

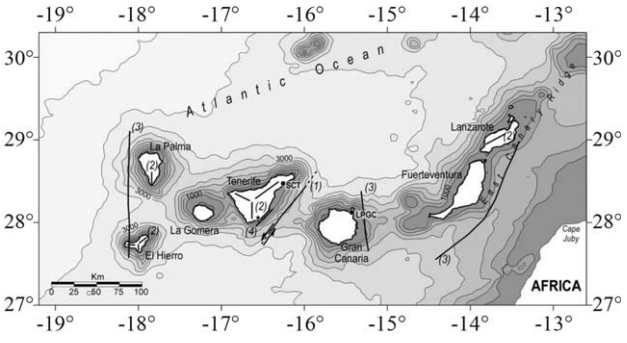

Figure 11 - Main tectonovolcanic features and lineations of the Canary Islands (González de Vallejo *et al.*, 2006). Numbers refer to the main works describing the structures shown in the figure: (1) Bosshard & McFarlane, 1970; Mezcua *et al.*, 1992; (2) Navarro, 1974; (3) Carbó *et al.*, 2003; (4) González de Vallejo *et al.*, 2003. Isolines show the bathymetry. The capital cities of the archipelago are displayed: Santa Cruz de Tenerife (SCT) and Las Palmas de Gran Canaria (LPGC). The star marks the location of the paleoliquefaction features.

6.3. Seismic data

The beginning of the historical period in the islands dates from the fourteenth century. Since then, a noticeable number of earthquakes have been registered, mainly related to volcanic eruptions (Fig. 12). The first great seismic event was registered on La Palma in 1677 (I_{MSK} = VII-VIII). However, the most intense earthquake in the archipelago took place near Yaiza (Lanzarote) in 1730 (I_{MSK} = X) related to the Lanzarote eruption (1730-1736) of the Timanfaya volcano. The so-called Yaiza earthquake took place on 1 September 1730 reaching an MSK intensity of X, however the intensity assigned to the Yaiza earthquake is very likely to be overestimated.

Other noticeable earthquakes were registered in 1920 and 1949 in Cumbre Vieja (La Palma) (I_{MSK} = VII), in Ingenio (Gran Canaria) in 1913 (I_{MSK} = VII), and in Fuerteventura in 1915 and 1917 (both I_{MSK} = VII). Many other events with intensity VI and V have been registered in the archipelago. The first seismic network in the region started operating in 1975. Since then most of the stations have been updated by digital recording broadband instruments (IGN, 2004).

The instrumental catalogue is mostly composed of small events distributed preferentially around Gran Canaria and Tenerife, in particular, between the two islands (Fig. 12). The largest instrumental earthquakes in the archipelago were recorded on 22 January 1991 and 9 May 1989. The 1991 event (m_bLg = 5.1) was located 60 km southwest of La Palma and no aftershocks were recorded, probably because of the long distance to the seismic network. In contrast, the 1989 event (m_bLg = 5.2) was located between Gran Canaria and Tenerife, permitting the record of a noticeable number of aftershocks. The hypocenter of the main shock was located by Dziewonski *et al.* (1990) at a depth of 15 km, whereas the IGN located it at a depth of 36 km, with an uncertainty in the focal depth of ± 12 km. The fault lo-

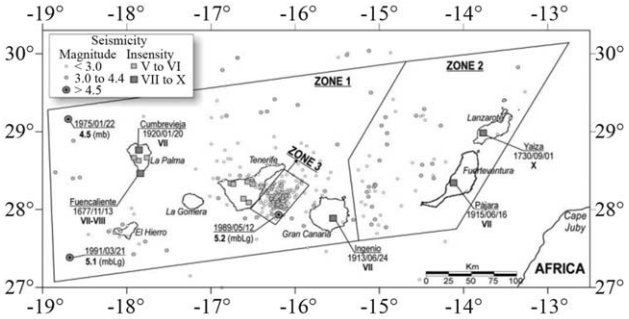

Figure 12 - Seismicity of the Canary Islands. Only historical events with intensity greater than V (MSK) are displayed. Only main events are labelled: name of the town, date and intensity for the historical events, and date and magnitude for the instrumental records. The seismogenic zones considered in the hazard calculations are shown. See text for details. (Gonzalez de Vallejo *et al.*, 2006).

cated between Gran Canaria and Tenerife was pointed out as the source of the 1989 event (Mezcua *et al.*, 1992). The focal mechanism of the main shock shows strike-slip movement with two nodal planes oriented north-northeast-south-southwest and northwest-southeast. The former agrees very well with the strike of the submarine fault and aftershock distribution. The length of the fault was estimated as 30 km.

6.4. Paleoseismic investigations

Paleoseismic investigations can provide very important seismic and tectonic information, especially in areas with few seismic records. One of its main contributions to seismic hazard is to identify possible earthquakes linked with active faults, although if liquefaction structures are identified in these studies, the acceleration due to the earthquake can also be estimated. Where possible, the age of the palaeo-earthquake can also be estimated.

Several structures attributed to liquefaction phenomena of seismic origin have been identified in exposed sand deposits near El Médano, on the south coast of Tenerife. Tectonic and geophysical investigations, geotechnical characterization, geochronological analysis, seismicity, and neotectonic data were carried out, as well as soil dynamic analysis (González de Vallejo *et al.*, 2003).

The liquefaction structures consist on clastic dikes and tubular vents. Their origin has being attributed to the liquefaction of sands by an earthquake of high intensity. The mechanisms that gave rise to the clastic dikes were hydraulic fracturing and lateral spreading of a layer of compact sands in response to high pore pressures of seismic origin (Fig. 13). These pressures, in turn, led to the movement and injection of sands across the compact sands level. The vents are the result of high upward hydraulic pressures causing the ejection of water and sand through these conduits to the surface, possibly forming sand blows and explosion craters (Fig. 14).

Figure 13 - Clastic dikes due to hydrofracturing by seismic shaking.

Figure 14 - Dikes showing a central aperture and a tabular vent.

The peak ground acceleration needed to produce liquefaction and the sand dikes was estimated at 0.22 to 0.35 *g* applying the Ishihara (1985), Obermeier (1996) and Obermeier *et al.* (2001) methods. An acceleration of 0.30 *g*, considered to be the most characteristic, would correspond to an intensity of VIII to IX at the site of liquefaction. The magnitude of the earthquake causing liquefaction was calculated to be in the range 6.4 to 7.2 with a value of $M = 6.8$ taken to be representative. This result was obtained assuming that a submarine fault (Figs. 11 and 12) was the seismic source.

The liquefaction structures developed over a tectonically uplifted beach of sand deposits dated as 10.081 ± 933 years BP. Over these sands and liquefaction structures, fine calcareous crust levels dated as 3490 ± 473 years BP were observed. The paleoearthquake responsible for liquefaction occurred during the Holocene; its age lying between these two dates. Nevertheless, tectonic and geomorphological data from field observations suggest an age closer to the younger constraint.

Possible seismic sources near the site of liquefaction were considered. The main source is inferred to have been a submarine NNE-SSW trending fault some 35 km from the site between the islands of Tenerife and Gran Canaria. Its movement takes the form of a sinistral thrust. This fault shows associated seismicity.

6.5. Seismogenic sources

Based on the main regional tectonic features and the distribution of seismicity, three seismogenic zones have been defined to be used in the hazard calculations: zones 1, 2 and 3 (Fig. 12). The area consisting of zones 1 and 2 accounts for the occurrence of low-to-moderate magnitude events, independent of their tectonic or volcanic origin. The boundaries of the zones have been drawn coinciding with the decrease in seismicity that occurs either toward the open Atlantic Ocean or toward the African continent, respectively (Fig. 12). The northern and southern limits of

these zones also follow the offshore extension of the Atlas structure (Figs. 11 and 12). The boundary between both zones represents the abrupt change in crustal thickness that takes place moving away from the eastern islands toward the western islands. The orientation of this boundary coincides approximately with the apparent north-northwest-south-southeast orientation displayed by the East Canary Ridge (Fig. 12).

Zone 3 has been defined to outline a specic area inside zone 1, between Gran Canaria and Tenerife, where moderate-to-large ($M_w > 6.0$) tectonic earthquakes are likely to occur due to the presence of the fault responsible for the 1989 sequence, and in accordance with the size of estimated earthquake magnitudes (M_w = 6.8) from paleoliquefaction analysis on the south Tenerife coast.

6.6. Seismic parameters for hazard calculations

Analyzing the temporal completeness of the database is of prime importance for estimating earthquake recurrence parameters in each seismogenic zone (Table 9).

Seismic hazard was calculated following the well-known method of Cornell (1968). This method assumes that earthquake occurrence follows a Poisson process and is distributed uniformly within several specic areas delimited by the analyst (source zones). In each of these zones, earthquake magnitudes fit an exponential distribution, so the mean annual exceedance rate of magnitude $m(\lambda_m)$ is given by (Cornell & Vanmarcke, 1969):

$$\lambda_m = \lambda_{m0} \frac{\exp(-\beta m) - \exp(-\beta m_1)}{\exp(-\beta m_0) - \exp(-\beta m_1)}, m_0 \le m \le m_1 \quad (6)$$

where λ_{m0} is the mean annual exceedance rate of magnitudes above m_0, and m_1 and m_0 are the upper and lower bounds of the distribution, respectively, and (β) is the exponential parameter of the distribution. The λ_{m0} parameter is given by:

$$\lambda_{m0} = \exp(\alpha - \beta m_0) \quad (7)$$

Table 9 - Estimated starting year of completeness for specic magnitude ranges.

Magnitude range (M_w)	Starting year	Temporal length (yr)
5.1-5.2	1850	153
4.1-5.0	1960	43
3.1-4.0	1975	28
2.6-3.0	1980 (zones 1 and 3) 1985 (zone 2)	23 18
2.0-2.5	1990	13

Temporal length extends from starting year to 2002.

where $\alpha = a$ Ln(10) and $\beta = b$ Ln(10), and a and b are the Gutenberg-Richter parameters. The Gutenberg-Richter parameters estimated in each zone after regression analysis are shown in Table 10. Zones 1 and 2 have shown a very different a value, which could be related to distinctive seismogenic characteristics. Nevertheless, this observation has to be taken with caution because of signicant statistical uncertainty affecting zone 2 parameters (Fig. 15).

Zone 3 represents a specic area inside zone 1 where earthquake occurrence is extended to larger magnitudes ($M_w \ge 6.0$) due to the presence of the Gran Canaria-Tenerife submarine fault. Hence, the maximum earthquake potential of zone 3 has been assessed based on the surface length of the Gran Canaria-Tenerife fault and paleoliquefaction evidence on the south coast of Tenerife. Making use of the surface rupture length versus moment magnitude relationship of Wells & Coppersmith (1994) and considering the 30 km length of the fault, an expected $M_w = 6.8 \pm 0.28$ event can be derived, which is very similar to the M_w = 6.8 estimated on the paleoliquefaction study of González de Vallejo *et al.* (2003). These authors estimated that such a seismic event occurred between 3,500 and 10,000 years ago, which is consistent with the mean recurrence period derived from extrapolating instrumental data to the large magnitude range (see Table 10).

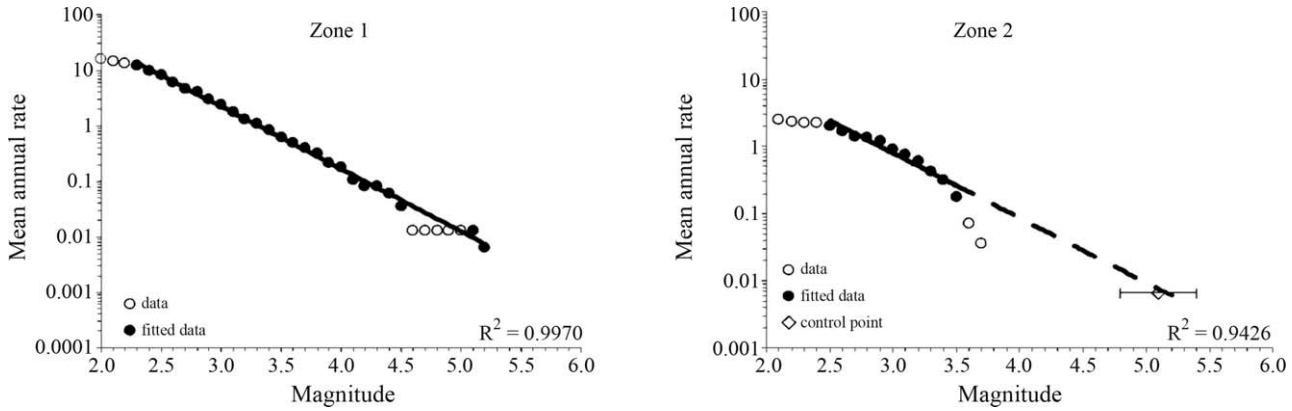

Figure 15 - Cumulative earthquake occurrence rates versus magnitude in zones 1 and 2, and exponential ts (González de Vallejo *et al.*, 2006).

Table 10 also shows the lower (m_0) and upper (m_1) magnitude thresholds adopted in zones 1 and 2. Minimum magnitude was set to M_w = 4.0 in zones 1 and 2. Standard practice in seismic-hazard assessment usually sets the minimum magnitude to M_w = 5.0, which is thought to be the smallest earthquake of engineering interest. Nevertheless, adopting such a value in a low-to-moderate seismic area like the Canary Islands, could lead to underestimating the hazard for relatively high exceedance probabilities (*e.g.* 10% in 50 yr or 475-yr return period). Besides, seismic events with magnitudes smaller than M_w = 5.0 have actually produced signicant damage in other parts of Spain.

To assess the maximum magnitude in zones 1 and 2, it was adopted a deterministic procedure of increasing the intensity of the maximum historical earthquake (MHE) by half a unit, and transforming it to the moment magnitude scale. MHEs in zones 1 and 2 are I_{MSK} = VIII and I_{MSK} = X, respectively. The former value suggests an average M_w = 6.0 with the relationships of IGN (1982) and Benito *et al.* (1999). In fact, adopting such intensity would indicate an average M_w = 6.8, which is no realistic if considering the maximum size of instrumentally recorded earthquakes related to major eruptions (Miyake-jima, 1983, M_S = 6.2; Oshima, 1986, M_w = 6.0; Benoit & McNutt, 1996). A maximum M_w = 6.0 was finally adopted for zone 2.

6.7. Ground-motion attenuation relationships

There is no ground-motion relationship specically developed for the Canary Islands. The only attenuation relationships derived for a similar volcanic archipelago to date are those developed by Munson & Thurber (1997) and Atkinson (2010) from Hawaiian strong-motion data. The Munson and Thurber equation was selected for the calculations. However, it is interesting to compare that relationship with the one of Ambraseys *et al.* (1996), which is one of the most used in Europe. Ambraseys *et al.* predicts higher PGA values for small-to-large magnitudes (M_S = 5.0-7.0) and at short distances (10 km approximately), Fig. 16. On the other hand, Munson and Thurber predict higher PGA in the medium distance range (10-100 km), although it attenuates much faster. These signicant differences between attenuation models suggest that the distinctive characteristics of active volcanic crust (*e.g.* fracturation, temperature, and uids) may produce a damping effect on high frequency ground motion, in particular, at short distances.

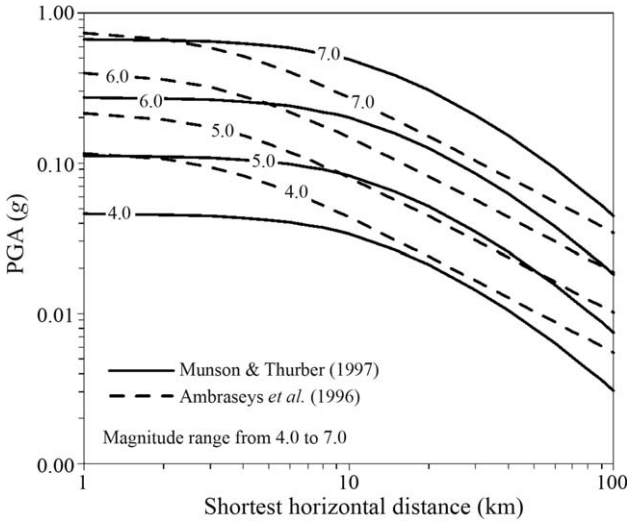

Figure 16 - Munson & Thurber (1997) PGA attenuation curves for M_w = 4.0 to 7.0 for rock conditions. The Ambraseys *et al.* (1996) curve is also shown for comparison purposes (González de Vallejo *et al.*, 2006).

6.8. Seismic-hazard results

Seismic hazard has been calculated for a grid spacing of 0.1°, as well as for the two capital cities (Las Palmas de Gran Canaria and Santa Cruz de Tenerife), (Gonzalez de Vallejo *et al.*, 2006). Computation was performed using the program CRISIS (Ordaz *et al.*, 1999). Figure 17 shows the seismic-hazard curve for the capital cities, and Fig. 18 (A and B) shows the resulting seismic-hazard maps in terms of PGA levels related to 475-and 950-yr return periods, respectively. PGA is for rock conditions, which are the most common site conditions on the islands. It is clear from both maps that zone 3 controls the distribution of the highest acceleration levels.

6.9. Conclusions

The east coast of Tenerife has been identied as the onshore area with highest seismic hazard in the archipelago because of the existence offshore east of Tenerife of a seismogenic source capable of generating moderate-to-

Table 10 - Seismic parameters of the seismogenic zones.

Sources	b	a	m_0	λm_0	m_1	MRP (yr)
Zone 1	1.12 (± 0.01)	3.72 (± 0.05)	4.0	0.1676	6.0	1,050 ± 120
Zone 2	0.95 (± 0.08)	2.75 (± 0.23)	4.0	0.0909	6.5	870 ± 160
Zone 3	1.12 (± 0.01)	3.72 (± 0.05)	6.0	0.00095	6.8	8,350 ± 950

a and b, Gutenberg-Richter parameters with indication of the standard error; m_0 and m_1, lower and upper bounds of magnitude (M_w) distribution; λm_0 mean annual cumulative rate of magnitude ≥ m_0; MRP, mean recurrence period of m_1 in each of the zones.

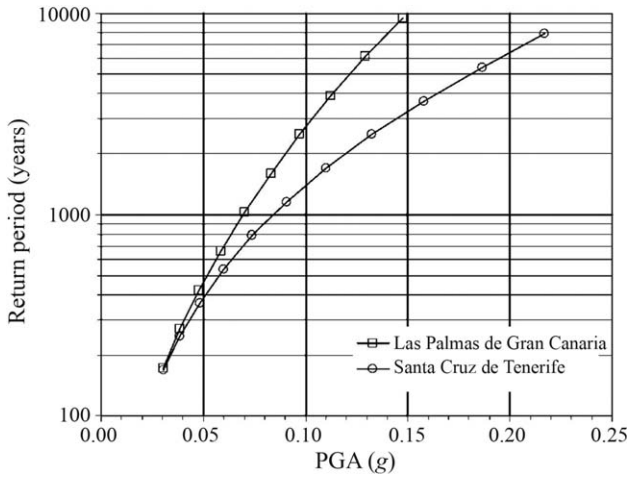

Figure 17 - Seismic-hazard curves for the two capital Canarian cities. PGA values are for rock conditions, (González de Vallejo *et al.*, 2006).

large magnitude ($M_w > 6.0$) tectonic earthquakes, that is, the Gran Canaria-Tenerife fault.

The eastern and south-eastern part of Tenerife show PGA values of 0.06 *g* and 0.08 to 0.09 *g* for the 475-and 950-yr return periods, respectively. The rest of the Canary Islands show a uniform PGA of 0.05 *g* for the 475-yr return period and 0.06 to 0.07 *g* for the 950-yr return period. PGA in the capital cities of Santa Cruz de Tenerife and Las Palmas de Gran Canaria are 0.06 and 0.05 *g*, respectively for the 475-yr return period, and 0.08 and 0.07 *g* for the 950-yr return period. These results on Tenerife and the rest of the Canary Islands are 50% and 25% higher than those stated in the Spanish Seismic Code (NCSE-02) for the 475-yr return period, respectively. Seismic Codes for building construction in the Canaries should be revised.

The presence of active faults affecting materials of very recent age and their association with a paleoearth-

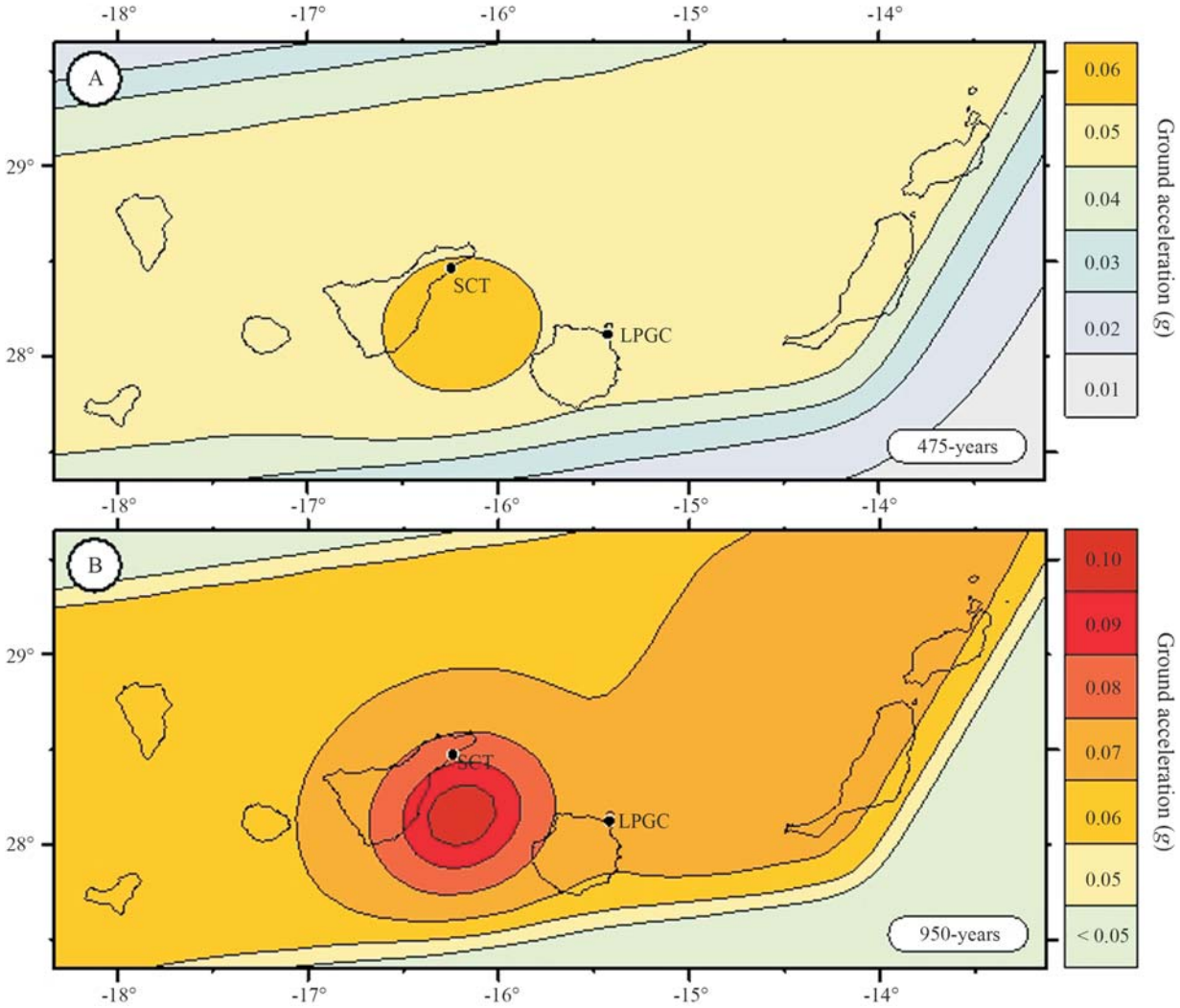

Figure 18 - Seismic-hazard maps of the Canary Islands in terms of PGA on rock for the 475 (A) and 950-yr (B) return period. Acceleration values are in *g* units (González de Vallejo *et al.*, 2006).

quake of high intensity in the south of Tenerife are key factors that need to be borne in mind when evaluating seismic hazards on the Canaries, a region which, up until now, had been considered to be of low tectonic seismic activity.

7. Large Landslides and Associated Tsunami Hazards: The Instability of the Volcanic Island Flanks of the Canary Islands Case Study

7.1. Introduction

The large landslides in the Canary Islands, have been the subject of many research studies although there was most scientific and social interest in them when alarming news was published on the possibility that the collapse of the island of La Palma could cause a catastrophic tsunami on the east coast of the US (Ward & Day, 2001). The resulting social alarm led to the start of an investigation into the causes of volcanic island flank instability in the Canaries, their failure mechanisms, and the possible associated hazards, particularly tsunamis. This investigation focused on two of the world's largest known landslides: the Güímar and La Orotava landslides in Tenerife (Ferrer *et al.*, 2008 and 2011, and Seisdedos, 2008).

Although more than 20 mega-landslides have been described in the Canary Islands affecting the flanks of the volcanic edifices, the Güímar and La Orotava landslides, (Fig. 19), originating 1 Ma and 0.6 Ma respectively, are two exceptional cases due to their huge dimensions and outstanding geomorphological features. Tsunami deposits have been also identified in some of the Canary Islands, probably associated with the landslide of the island flanks.

The presence of large masses of rocks and debris avalanche deposits lying on the sea bed surrounding the island of Tenerife is the main evidence of the Güímar and La Orotava landslides. According to Acosta *et al.* (2003) La Orotava submarine debris avalanche deposits cover an area of 2,200 km^2 reaching up to 75 km from the coast, and the submarine deposits from the Güímar landslide occupy an area of 2,600 km^2 up to a distance of 85 km from the coast. The volume of these debris avalanches on the ocean floor has been estimated at around 120 km^3 in the case of the Güímar landslide and less than 500 km^3 in La Orotava (Masson *et al.*, 2002).

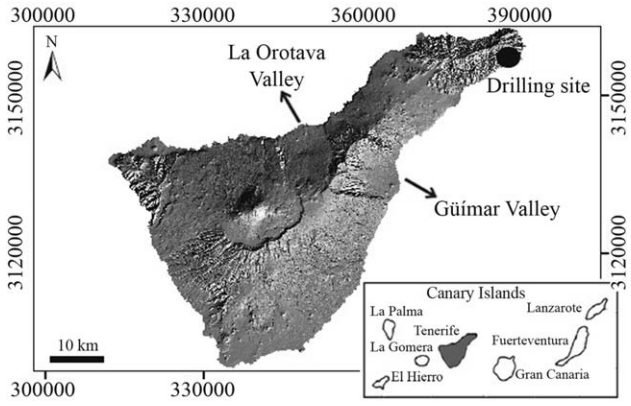

Figure 19 - Location of Güímar and La Orotava valleys and drilling site, Tenerife.

The morphological characteristics of the valleys are extraordinary, with their outstanding symmetry and the important height of the lateral scarps (more than 500 m in some areas; Fig. 20), cut in pre-landslide volcanic materials with slope angles higher than 35°. The depressions formed by the landslides were filled with post-landslide volcanic materials, mainly lava flows from new volcanoes in the upper part of the valleys, with slope angles currently lower than 15°. The estimated volume of the landslide rocks from the volcanic flanks, calculated roughly from the depressions created by the rockslides, is of the order of 70-100 km^3 each.

7.2. Geological and geomechanical model

Geological and geotechnical data were recorded from field surveys and in the extensive network of small diameter galleries, with a total length of over 1,000 km, excavated for groundwater supply purposes. The geotechnical properties of the volcanic materials of the emerged edifice have been also obtained from in-situ and laboratory tests (González de Vallejo *et al.*, 2008; Seisdedos, 2008).

With regard to the geological and geomechanical data of the submarine edifice, only morphological and tectonic data are available from marine geological and bathymetric surveys. In the north-eastern corner of the island site investigations have been carried out where the submarine rock outcrops (Fig. 19). Three boreholes have been drilled in hyaloclastites with one of them reaching a depth of 200 m.

Nine lithological units have been described as representative of the island flanks and the structural axis of the pre-rockslide edifice as shown in Fig. 21. These units have been differentiated following engineering geological criteria:

Figure 20 - View of La Orotava valley, 12 km wide, bordered by 500 m high lateral scarps. In the background El Teide volcano (3,718 m).

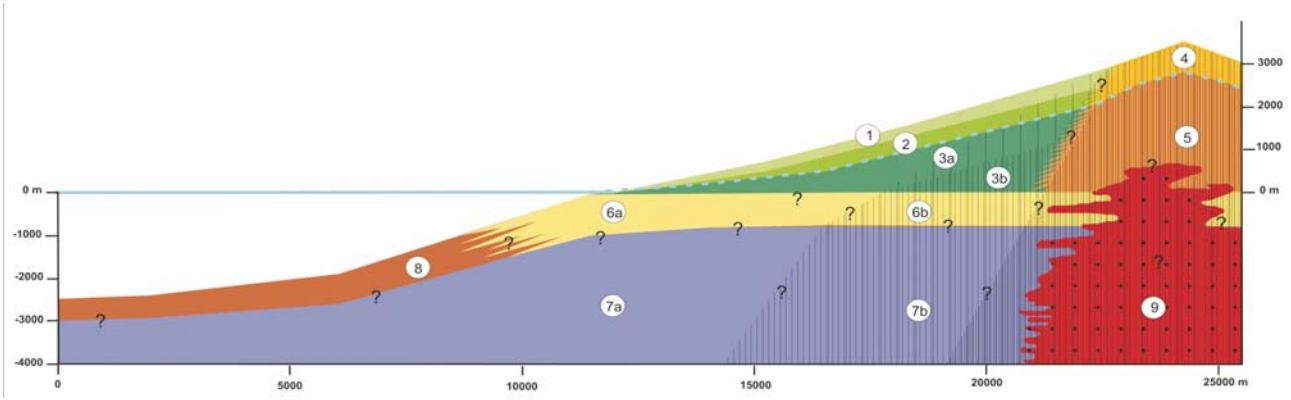

Figure 21 - Geological and geomechanical model representative of the pre-landslide volcanic edifice of Güímar and La Orotava landslides (Ferrer *et al.*, 2008). Dashed blue line: water level; question marks: uncertainties.

- Unit 1: Recent lava flows with scoria layers, with a low degree of alteration, interbedded lenses of loose scoria and cavities.
- Unit 2: Slightly altered lava flows with scoria layers; lower presence of cavities than Unit 1.
- Unit 3: Altered lava flows and highly compacted pyroclastic layers with intense dike intrusion.
- Unit 4: Pyroclasts and lava flows with scoria, low alteration, high compaction and intense dike intrusion.
- Unit 5: Pyroclasts and altered lava flows, with very intense dike intrusion, highly compacted and fractured.
- Unit 6: Hyaloclastite rocks from subaerial flows as well as from submarine eruptions.
- Unit 7: Pillow-lavas from submarine eruptions representing the main phase of submarine growth of the island.
- Unit 8: Deposits from gravitational slides on the submarine island flanks.
- Unit 9: Dikes and plutonic complex.

A summary of geomechanical properties corresponding to the rock units is shown in Table 11.

From these 9 units, hyaloclastite rocks (unit 6) are a rare rock type not only from the mineralogical and fabric point of view but also because of their unusual geomechanical properties. However, very few geotechnical studies have been carried out on this type of rock.

Hyaloclastites are composed of clastic particles of irregular shape with sizes ranging from 0.5 to 3 cm, forming a green, grey or brown coloured breccia (Fig. 22). This material is poorly consolidated and weakly cemented. Voids and vacuoles with sizes from 0.5 to 3 cm are occasionally present. Secondary minerals are observed inside them. Fracture zones and slickenside surfaces have been identified.

The deformational properties of the hyaloclastite rock mass were obtained from 16 pressuremeter tests carried out at different depths in boreholes. Pressuremeter module values ranged from 50 MPa to 3,200 MPa, with mean representative values of 560 MPa. Table 12 shows some mechanical properties of the hyaloclastites obtained from laboratory tests.

7.3. Stability conditions of the pre-failure edifice

Stability analysis was carried out on the pre-failure edifices of the Güímar and La Orotava valleys applying limit equilibrium and stress-strain methods (Ferrer *et al.*, 2011). A first analysis was developed using rock mass pa-

Table 11 - Geomechanical indexes and properties of volcanic rocks.

Material	RMR*	GSI*	σ_{ci} (MPa)	γ_{dry} (kN/m^3)	γ_{sat} (kN/m^3)
Lava flows in massive layers	57-68	52-63	98	24	25
Lava flows and scoria layers	-	14-25	34	15	16
Altered lava flows	44-55	39-50	46	17	18
Pyroclasts	-	9-20	2	12	14
Dikes	55-70	50-65	175	27	28
Hyaloclastite rocks	-	10-21	6	21	24
Pillow-lavas	63-68	58-63	150	27	28

*The lower values of intervals correspond to materials below water table.
RMR = rockmass rating, GSI = Geological strength index, σ_{ci} = uniaxial compressive strength, γ_{dry} = dry unit weight, γ_{sat} = saturated unit weight.

Figure 22 - Hyaloclastite rock cores.

Table 12 - Hyaloclastite intact rock properties.

Property	Mean values
Unit weigh	23-29 kN/m^3
Uniaxial strength	16 MPa
Tensile strength	1.5-1.8 MPa
Young modulus	4,300 MPa
Poisson coefficient	0.27-0.31
Strength parameters c, ϕ	3-5 MPa; 43-50°

rameters obtained from the application of Hoek-Brown failure criterion (Table 13). Figure 23 gives the results of the analysis showing a deformational pattern affecting the whole edifice. In this case the factor of safety is higher than 1.3. A second stability analysis was carried out to obtain the strength values for the hyaloclastites for limit equilibrium conditions. Figure 24 shows the results obtained. In this case, the strain distribution shows larger deformations affecting the hyaloclastites and defining a complex failure surface. Values of 0.1 MPa for cohesion and 16° for angle of friction were obtained to reach limit equilibrium conditions.

Table 13 - Strength and deformation properties obtained for the units of the pre-failure edifice using Hoek and Brown criterion.

Unit	c (MPa)	ϕ (°)	E (MPa)
1	0.9	51	6,750
2	1.7	47	8,920
3a	2.3	34	4,200
3b	3.1	25	2,780
4	0.9	33	2,300
5	2.8	22	2,050
6a	1.5	30	1,010
6b	2.5	35	1,170
7a	8.0	36	12,020
7b	11.4	34	13,180
8	1.0	20	1,000
9	13.2	33	10,230

A multiple successive failure mechanism was also analysed. The results are shown in Fig. 25. A critical factor of safety (near or lower than 1.00) is obtained for this type of failure mechanism. Potential failure surfaces are obtained from these results that are in accordance with the geomorphological and geological features observed in the Güímar and La Orotava valleys, as well as with the geomechanical properties of the materials involved (Ferrer *et al.*, 2010).

7.4. Uncertainty analysis

The uncertainties in the stability model of the island edifices were analysed by logic tree methods. To identify sources or larger uncertainties a preliminary analysis was carried out at the early stages of the project, before site investigations. The results showed that the geomechanical properties of the hyaloclastite submarine rocks rated the highest uncertainty values (63%). A second uncertainty analysis was carried out after site investigation on the submarine rocks. The uncertainties were reduced to 21%. Several logic trees were developed for each factor contributing to flank stability. Figure 26 gives an example, showing the uncertainty value of 39% for flank stability before site investigation. After site investigation this value was reduced to 26%.

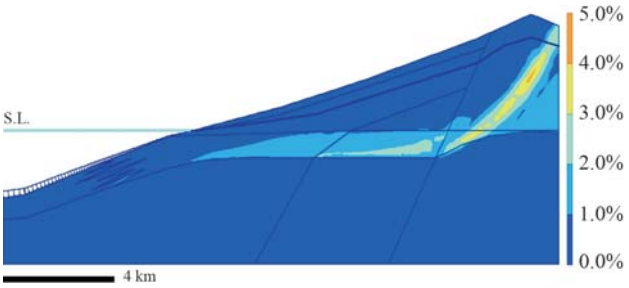

Figure 23 - Deformational model from the stability analysis using Table 13 data. Horizontal scale = vertical scale.

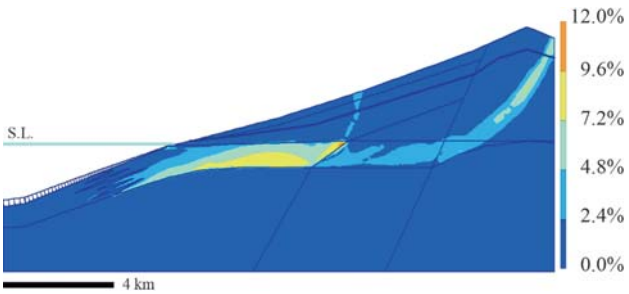

Figure 24 - Deformational model for the initiation of failure (FS = 1.0) and strength values for hyaloclastite rocks: c = 0.1 MPa and ϕ = 19°. Horizontal scale = vertical scale.

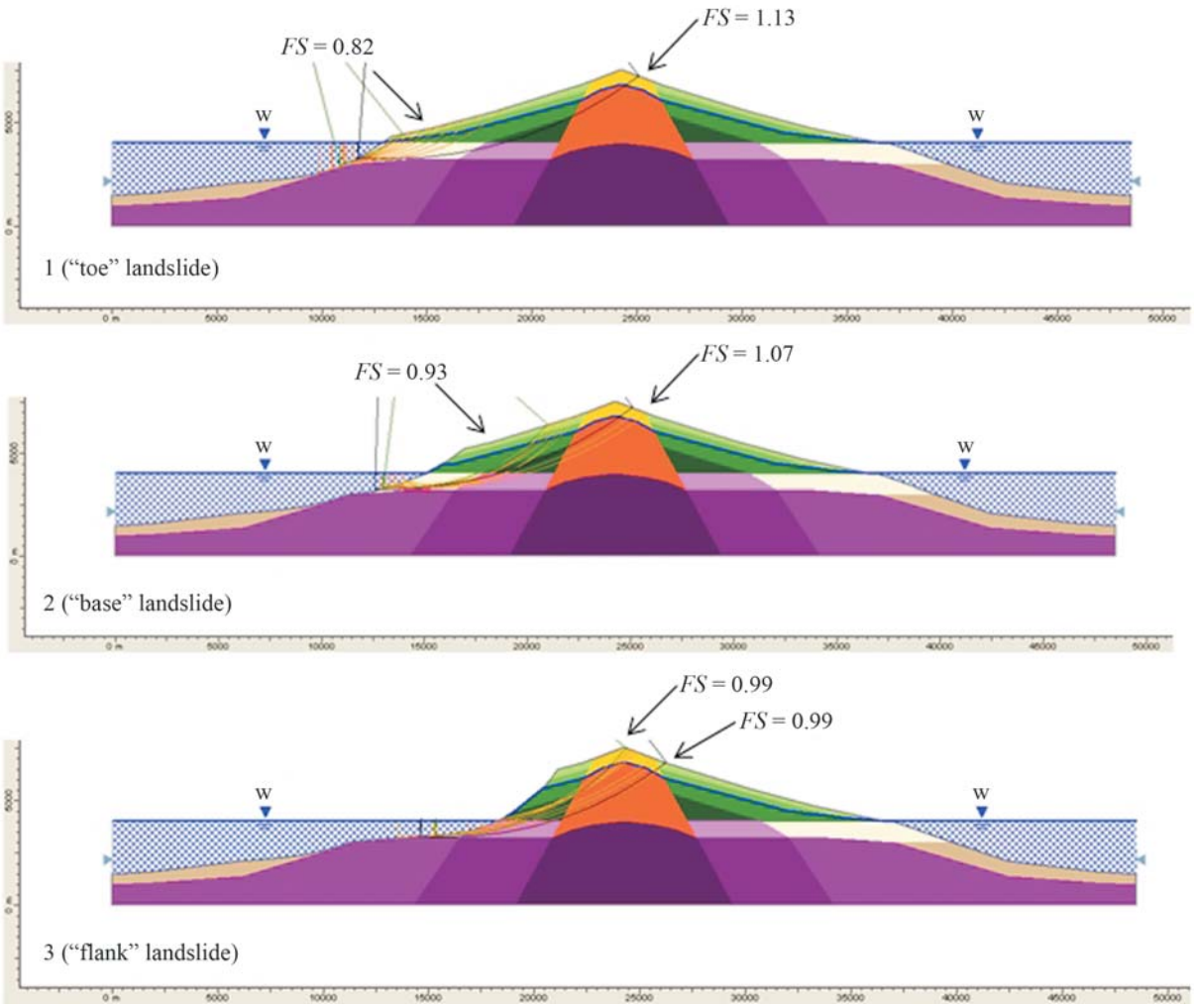

Figure 25 - Successive failure mechanism analysis for the volcanic flanks of Tenerife.

7.5. Tsunami deposits

Tsunami deposits have been identified in Teno (Tenerife), Piedra Alta (Lanzarote) and Agaete (Gran Canaria) (Fig. 27). The Agaete deposits have been described by Pérez Torrado *et al.* (2002) and Madeira *et al.* (2011). At least 3 different tsunami events have been identified over the last 2 Ma. Some sedimentological features of these deposits are shown in Fig. 28. Paleontological and paleoclimatic investigations indicate an age between 1.8 to 2.0 Ma (Meco *et al.*, 2008).

The Teno tsunami deposits, in Tenerife (Fig. 29), are probably associated with the flank collapse of El Teide volcanic pre-edifice or Cañadas Edifice, c. 150-180 ka. The Piedra Alta tsunami deposits, on the island of Lanzarote (Fig. 30), contain many specimens of marine fauna. An age of c. 330 ka has been attributed, based on paleoclimatic and paleontological criteria (Meco *et al.*, 2008).

The sedimentological characteristics of all these deposits indicate a high energy source and a high speed mechanism of the landslide materials entering the sea. Although the tsunami sources are still being investigated, a relationship with the large landslides occurring in the Canary Islands during the Pleistocene is the most probable origin.

The possible run-up of the largest waves of these tsunamis may have exceeded a height of 50 m at the Agaete and Teno sites, and of at least 25 m at the Piedra Alta site, as deduced from the location of the deposits today and sea level changes during the last 2 Ma.

Figure 27 shows the location of tsunami deposits and potential landslide source areas. More absolute dating measurements are needed to establish direct relationships between specific landslides and tsunami deposits.

7.6. Conclusions

The instability of the pre-failure edifices of the island flanks of Güimar and La Orotava, originated when a critical height of the island and a critical slope angle were reached. Flank instability was initiated under the sea where hyaloclastite rocks are present with low strength and high deformability properties, playing a fundamental role in sta-

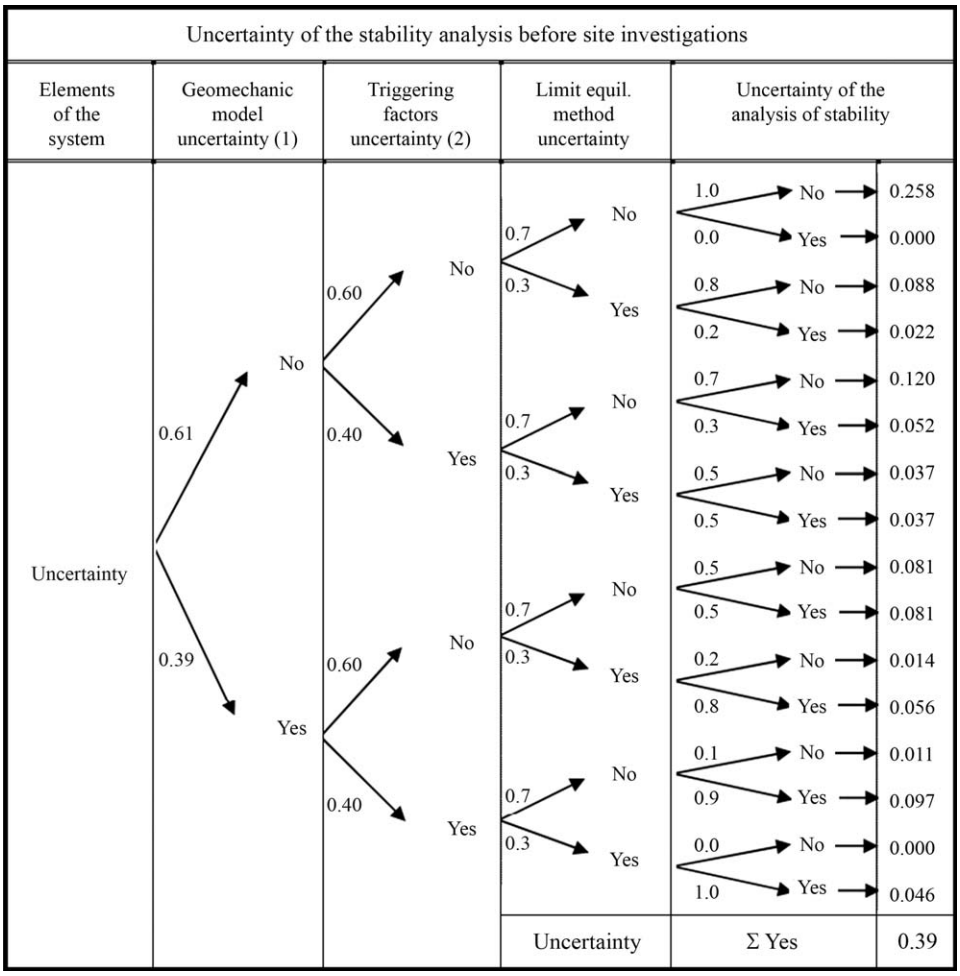

Figure 26 - Uncertainties of the stability analysis before site investigations were carried out by logic tree methods (Seisdedos, 2008). 1 and 2: uncertainties of the geomechanical model and the triggering factors, respectively, using additional logic trees results.

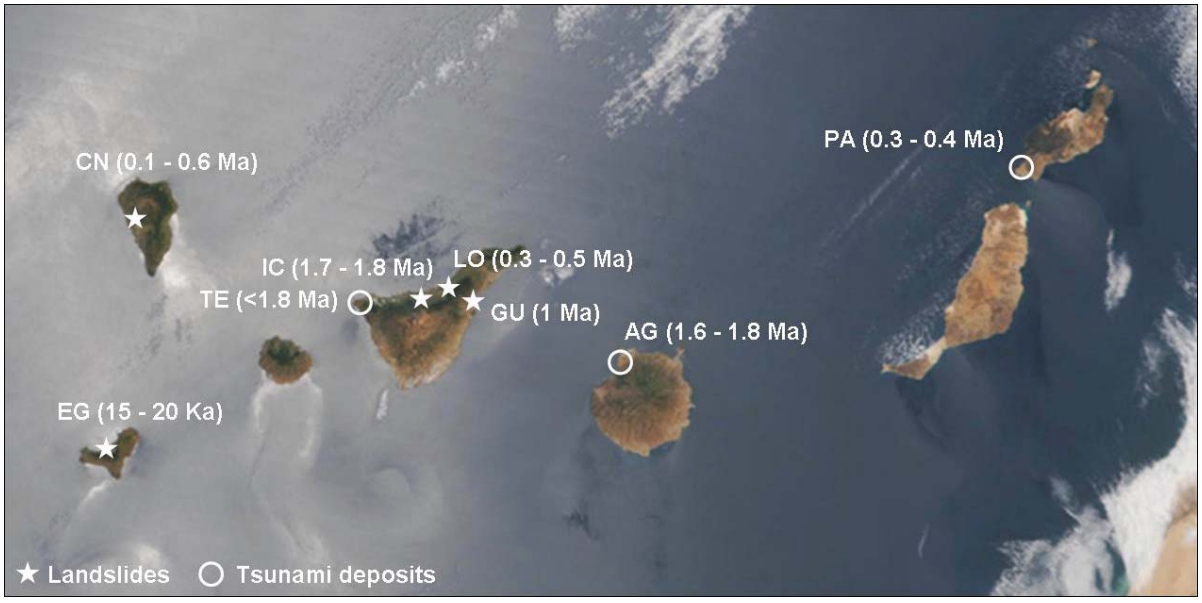

Figure 27 - Large paleo-landslides and tsunami deposits in the Canary Islands. Landslides: CN- Cumbre Nueva (La Palma), EG- El Golfo (El Hierro), IC: Icod, LO: La Orotava (Tenerife), GU: Guímar (Tenerife). Tsunamis: TE- Teno (Tenerife), AG- Agaete (Gran Canaria), PA- Piedra Alta (Lanzarote).

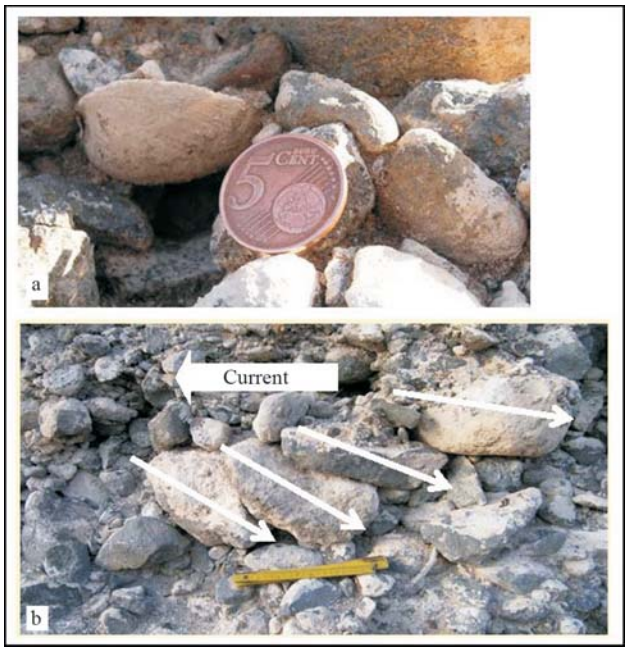

Figure 28 - Agaete tsunami deposits with *glycimeris* shells fossils and imbricated flat boulders showing paleo-current direction (photos from J. Madeira).

Figure 29 - Tsunami deposits in Teno, northwest coast of Tenerife (area shown 2 m height).

bility. Other contributing factors to flank instability include volcanic activity and seismic shaking. The instability process may have generated several large landslides and associated tsunamis. The tsunami deposits identified on several islands suggest a very rapid mass movement of rocks and debris falling into the sea with a high energy impact. Tsunami waves may have reached a height of over 50 m and may have been propagated to neighbouring islands many km away from the tsunami sources. Landslides are natural building and dismantling processes on volcanic islands, and are present not only in the Canary Islands but in many other islands worldwide, *e.g.* Hawaii, Fogo in Cabo Verde and Reunion.

Figure 30 - Piedra Alta tsunami deposits located in the southwest coast of Lanzarote (area shown 2.5 m height).

At least 3 mega-landslides have occurred in Tenerife in the last 1 Ma being the recurrent time of tsunamis generated by these large landslides of some hundreds of thousands of years. On the other hand, Eff-Darwich *et al.* (2010), estimate a recurrent time from El Teide (Tenerife) and Cumbre Vieja (La Palma) flank collapses over 130,000 years.

8. Concluding Remarks

In the previous sections 3 case studies have been analysed as examples of the Engineering Geological Method (EGM) applied to geo-hazard assessment for engineering and territorial planning purposes. Different types of geo-hazards, including landslides on geotechnical and geological scales, earthquakes, tsunamis and induced seismicity, have been considered. The most significant results are summarised in Tables 14, 15 and 16.

Fifteen different types of methodologies have been used in the 3 cases (Table 14), 6 of these common to all cases:

- Geological surveys
- Geomorphologic and remote sensing studies
- Tectonic and active faulting investigations
- Geochronology and absolute dating
- Geotechnical site investigations
- Statistical and probabilistic analysis.

Table 15 shows the most relevant results: in case 1 and case 3, the extremely low probability of the geo-hazards analysed practically rules out any risk; however, in case 2, the earthquake resistant building standards for the region underestimate the seismic hazard.

Social acceptability has been compared before and after hazard assessment results (Table 16). These results point out the importance of the EGM approach to social acceptability. According with the criteria shown in Table 5, social acceptability to risks in the cases analysed can be

classified as follow: acceptable (I) for case 1 and case 3, and acceptable with restrictions (II) for case 2.

To conclude, the following aspects can be highlighted:

- Engineering Geological Methodology (EGM) is a practical tool for geo-hazard and risk assessment when engineering or planning design decisions have to be considered. This approach integrates different methodologies and procedures from geological, geo-engineering, statistic and probabilistic and engineering sciences.
- Applying EGM to the case studies analysed has resulted in the following engineering decisions and social implications:
  - Itoiz dam is safe for the geo-hazards considered. Social alarm has subsided and legal and political actions have been cancelled.
  - The extremely low probability of mega-landslides and tsunamis rules out any practical consideration of these for engineering and urban planning purposes in the Canary Islands.
  - Earthquake resistant standards for building construction in the Canary Islands underestimate the seismic hazard and should be revised.

Table 14 - Engineering geological methods used in the case studies analysed for hazard assessment.

Type of studies, surveys and methods	Case 1	Case 2	Case 3
Geological surveys	X	X	X
Geomorphological and remote sensing	X	X	X
Sedimentological, petrological and mineralogical investigations	-	X	X
Tectonic and active faulting studies	X	X	X
Geochronology and absolute dating	X	X	X
Paleontological studies	-	-	X
Geotechnical site investigation	X	X	X
Land geophysics	X	-	-
Marine geophysics	-	X	X
Geotechnical instrumentation	X	-	-
Geotechnical modelling and analysis	X	-	X
Seismicity studies	X	X	-
Paleo-seismological investigation	-	X	-
Historical records	-	X	-
Statistical and probabilistic analysis	X	X	X

Case 1: Itoiz dam. Case 2: regional seismic hazards. Case 3: landslides and tsunamis.

Table 15 - Results of the application of engineering geological methods to geo-hazard assessment.

Case study	Case 1 Itoiz dam safety	Case 2 Regional seismic hazards		Case 3 Landslides and tsunamis hazards	
Type of hazard	Slope instability	Earthquake hazard	Seismic hazard	Large landslides	Tsunamis
Size	$3x10^6$ m^3 landslide volume	Max. event during reservoir filling $M = 4.6$	Max. historic event $I = IX$ Max. instrumental event $M = 5.2$	Some of the largest in the world by volume	Large tsunamis affecting the Canary Islands coasts
Frequency	3 landslides from 38 ka to 12 ka ago	Probable EQ $M = 5.1$	Moderate to low magnitude EQ for 500 to 1,000 years RP	Over 20 landslides during last 2 Ma	Tsunamis associated to large landslides
Maximum potential events	Non active for the last 12 ka	EQ from potential active fault $M \approx 6.5$	EQ from potential active fault $M = 6.8$ EQ from paleoseismic data PGA ≈ 0.22-0.35	> 100 km^3 volume	Tsunamis run up waves 50 m height
Hazard assessment	$FS > 1.6$-500 yr RP $FS > 1.5$-1,000 yr RP $FS > 1.1$-5,000 yr RP	PGA 0.08 *g* - 500 yr RP PGA 0.12 *g* - 1,000 yr RP PGA 0.30 *g* - 5,000 yr RP	PGA 0.06 *g* - 500 yr RP PGA 0.08 *g* - 1,000 yr RP	$p < 10^{-5}$	$p < 10^{-5}$
Engineering implications	No risk even for extreme events		Conventional buildings at risk in zones with PGA values ≥ 0.05 *g*. Seismic codes should be revised	No risk for either infrastructures nor territorial planning	

M = magnitude; *I* = intensity; EQ = earthquake; RP = return period; PGA = peak ground acceleration; *FS* = factor of safety; *p* = probability of occurrence.

Table 16 - Social acceptability and economical impact of the case studies analysed.

Case study	Before hazard assessment	After hazard assessment
Case 1 Itoiz dam safety	Social opposition to dam construction. Negative economic impact.	No social opposition. Dam operating normally. Positive economic impact.
Case 2 Regional seismic hazard	Social concern even with low magnitude earthquakes.	Social and professional demands on revision building seismic codes.
Case 3 Landslides and tsunamis	Social alarm. High impact on media. Increase if insurance costs. Negative tourism impact.	No social alarm. No tourist concern.

- Although codes and regulations can state design criteria for different hazard scenarios, the society will not accept the risk of failure or its environmental consequences in the short, medium or long term, therefore engineering projects should provide not only design parameters, but also include scientific criteria that prove that the project solutions are socially acceptable.

Acknowledgments

The author is very grateful to the Portuguese Geotechnical Society and Association of Geotécnicos Antigos Alunos da Universidade Nova de Lisboa to be invited to present the XXVII Manuel Rocha Lecture. He is indebted to his colleagues who have contributed to the results presented in this paper, in particular to Dra. Mercedes Ferrer, Dra. Julia Seisdedos, Angel Rodriguez Franco, Dr. Juan Miguel Insua, Dr. Julian Garcia Mayordomo, Juan Jesus Coello, Jose Manuel Navarro, Dr. Jose Antonio Rodriguez Losada, Juan Carlos Garcia Davalillo, Luis Enrique Hernandez, Prof. Cesar Andrade, Dr. Jose Madeira, Dra. Conceiçao Freitas, Prof. Ramón Capote and Luis Cabrera. The author gratefully acknowledges the cooperation of Rene Gomez and Raimundo Lafuente and the assistance of Beatriz Blanco in the preparation of this paper.

References

Acosta, J.; Uchupi, E.; Muñoz, A.; Herranz, P.; Palomo, C. & Ballesteros, M. (2003) Geologic evolution of the Canarian Islands of Lanzarote, Fuerteventura, Gran Canaria and La Gomera and comparison of landslides at these island with those at Tenerife, La Palma and El Hierro. Mar. Geophys. Res., 24:1-40.

Ambraseys, N.N.; Simpson, K.A. & Bommer, J.J. (1996) Prediction of horizontal response spectra in Europe. Earthquake Eng. Struct. Dynamics, 25:371-400.

Atkinson, G.M. (2010) Ground motion prediction equations for Hawaii from a referenced empirical approach. Bull. Seism. Soc. Am., 100:751-761.

Banda, E.; Danobeitia, J.J.; Suriñach, E. & Ansorge, J. (1981) Features of crustal structure under the Canary Islands. Earth Planet. Sci. Lett., 55:11-24.

Benito, B.; Cabañas, L.; Jiménez Peña, M.E.; Cabañas, C.; Álvarez Rubio, S.; López Arroyo, L.; Ramírez, M.S. & Nuche, R. (1999) Caracterización Sísmica de Emplazamientos de la Península Ibérica y Evaluación del Daño Potencial en Estructuras. Proyecto Daños. Consejo de Seguridad Nuclear, Madrid, 240 pp.

Benoit, J.P. & McNutt, S.R. (1996) Global volcanic earthquake swarm database 1979-1989. U.S. Geol. Surv. Open-File Rep., 96-69, 32 pp.

Bommer, J.J.; Scherbaum, F.; Bungum, H.; Cotton, F.; Sabetta, F. & Abrahamson, N.A. (2005) On the use of logic trees for ground-motion prediction equations in seismic hazard analysis. Bull. Seism. Soc. Am., 95:377-389.

Bosshard, E. & MacFarlane, D.J. (1970) Crustal structure of the westerm Canary Islands from seismic refraction and gravity data. J. Geophys. Res., 75:4901-4918.

Carbó, A.; Muñoz-Martín, A.; Llanes, P.; Álvarez, J. & ZEE Working Group (2003) Gravity analysis offshore the Canary Islands from a systematic survey. Mar. Geophys. Res., 24:113-127.

CETS (Commission on Engineering and Technical System) (1995) Probabilistic Methods in Geotechnical Engineering. National Research Council, Washington, D.C., 95 pp.

Cornell, C.A. (1968) Engineering seismic risk analysis. Bull. Seism. Soc. Am., 58:1583-1606.

Cornell, C.A. & Vanmarcke, E.H. (1969) The major influences on seismic risk. Proc. Fourth World Conference on Earthquake Engineering, Santiago, v. 1, pp. 69-83.

Dziewonski, A.M.; Ekström, G.; Woodhouse, J.H. & Zwart, G. (1990) Centroid-moment tensor solutions for April-June 1989. Phys. Earth Planet. Int., 60:243-253.

Eff-Darwich, A.; García-Lorenzo, B.; Rodríguez-Losada, A.; de la Nuez, J.; Hernandez-Gutierrez, L.E. & Romero-Ruiz, M.C. (2010) Comparative analysis of the impact of geological activity on the structural design of the telescope facilities in the Canary Islands, Hawaii and Chile. Mon. Not. R. Astron. Soc., 407:1361-1375.

Fenton, G.A. & Griffiths, D.V. (2008) Risk Assessment in Geotechnical Engineering. John Wiley & Sons, New York, 461 pp.

Ferrer, M.; González de Vallejo, L.; Seisdedos, J.; Coello, J.J.; García, J.C.; Hernandez, L.E.; Casillas, R.; Martín, C.; Rodríguez, J.A.; Madeira, J.; Andrade, C.; Freitas, C.; Lomoschitz, A.; Yepes, J.; Meco, J. & Betancort, J.F. (2011) Güimar and La Orotava landslides (Tenerife) and tsunami deposits in Canary Islands. Proc. 2nd World Landslide Forum, Roma, Springer. (In press).

Ferrer, M.; Seisdedos, J. & González de Vallejo, L.I. (2010) The role of hyaloclastite rocks in the stability of the volcanic island flank of Tenerife. Olalla, C.; Hernández, L.E.; Rodríguez-Losada, J.A.; Perucho, A. & González-Gallego, J. (eds), Volcanic Rock Mechanics. Taylor and Francis Group, London, v. 1, pp. 167-170.

Ferrer, M.; González de Vallejo, L.I.; Seisdedos, J.; García, J.C.; Coello Bravo, J.J.; Casillas, R.; Martín, C. & Hernández, L.E. (2008) Large rockslides hazards in Tenerife island. Geological analysis and geomechanical modeling of instability mechanism. Proyecto CGL2004-00899, Instituto Geológico y Minero de España, Madrid, 340 pp.

Gomes Coelho, A. (2005) O problema das falhas activas na engenharia civil. Número especial XXII Liçao Manuel Rocha. Geotecnia, 105:13-67.

González de Vallejo, L. & Ferrer, M. (2011) Geological Engineering. CRC Press / Balkema, 678 pp.

González de Vallejo, L.; Rodriguez Franco, J.A.; Seisdedos, J.; Insua, J.M., García-Mayordomo, J.; Blazquez, R. & López Queirol, S. (2009) Análisis y Seguimiento del Embalse de Itoiz: Estabilidad de Laderas, Sismicidad y Condiciones Geotécnicas. Plan Nacional de Investigación Científica, Ministerio de Medio Ambiente, Madrid, 1056 pp.

González de Vallejo, L.I.; Hijazo, T. & Ferrer, M. (2008) Engineering geological properties of the volcanic rocks and soils of the Canary Islands. Soils and Rocks, 31:3-13.

González de Vallejo, L.I.; García-Mayordomo, J. & Insua, J.M. (2006) Probabilistic seismic hazard assessment of the Canary Islands. Bull. Seism. Soc. Am., 96:2040-2049.

González de Vallejo, L.; Rodriguez Franco, J.A.; Insua, J.M. & García-Mayordomo, J. (2005) Informe de supervisión de los estudios y análisis disponibles sobre la seguridad de la Presa de Itoiz. Ministerio de Medio Ambiente, Colegio Oficial de Geólogos de España, Madrid, 110 p. www.icog.es and downloader on January 1fst 2012.

González de Vallejo, L.I.; Capote, R.; Cabrera, L.; Insua, J.M. & Acosta J. (2003) Paleoliquefaction evidence in Tenerife (Canary Islands) and possible seismotectonic sources. Mar. Geophys. Res., 24:149-160.

González de Vallejo, L. (1994) Seismotectonic hazard for engineering projects in moderate seismicity regions. Proc. 7th. Int. Congress of Eng. Geology, Lisbon, Keynote Lecture Volume, pp. XIX-XXXVIII.

Gupta, H.K. (2002) A review of recent studies of triggered earthquakes by artificial water reservoirs with special emphasis on earthquakes in Koyna, India. Earth-Sciences Reviews, 58:279-310.

Gutierrez, F.; Lucha, P. & Galve, J.P. (2007) Cartografía geomorfológica del entorno del embalse de Yesa. Confederación Hidrográfica del Ebro, Zaragoza, 35 pp.

Hoek, E. (1991) When is a design in rock engineering acceptable? Proc. 7th Int. Conf. on Rock Mechanics. ISRM. Aachen, Germany, v. 3, pp. 1485-1497.

Instituto Geográfico Nacional (IGN) (1982) Catálogo General de Isosistas de la Peninsula Ibérica. Publicación 202. Instituto Geográfico Nacional, Madrid, 323 pp.

Instituto Geográfico Nacional (IGN) (2004) Seismic Network and Stations. Instituto Geográfico Nacional, Madrid, www.geo.ign.es on january 1fst 2012.

Ishihara, K. (1985) Stability of material deposit during earthquakes. Proc. 11 th. Int. Conf.Soil. Mech. and Found. Eng. San Francisco. A.A. Balkema, Rotterdam, v. 1, pp. 321-376.

Madeira, J.; Ferrer, M.; González de Vallejo, L.I.; Andrade, C.; Freitas, M.C.; Lomoschitz, A. & Hoffman, D. (2011) Agaete revisited: new data on the Gran Canaria tsunamiites. Geophysical Research Abstracs. European Geosciences Union (EGU). General Assambly, 13:2292-2294.

Masson, D.G.; Watts, A.B.; Gee, M.J.R.; Urgeles, R.; Mitchell, N.C.; Le Bas, T.P. & Canals, M. (2002) Slope failures on the flanks of the western Canary Islands. Earth Sci. Rev., 57:1-35.

McGarr, A.; Simpson, D. & Seeber, L. (2002) Case histories of induced and triggered seismicity. Lee, W.H.K.; Kanamori, H.; Jennings, P.C. & Kisslinger, C. (eds) International Handbook of Earthquake and Engineering Seismology, Part A. Academic Press, New York; pp. 647-661.

McHarg, I.L. (1969) Design with Nature. The American Museum of Natural History, New York, 198 pp.

Meco, J. (2008) Paleoclimatología del Neógeno en las Islas Canarias - Pleistoceno y Holoceno. Ministerio de Medio Ambiente, Madrid, 204 pp.

Mezcua, J.; Burforn, E.; Udías, A. & Rueda, J. (1992) Seismotectonic of the Canary Islands. Tectonophysics, 208:447-452.

Mogi, K. (1963) Some discussion on aftershock, foreshocks and earthquake swarms. The fracture of a semi-infinite body caused by a inner stress origin and its relation to the earthquake phenomena. Bull. Earth. Res. Inst., 41:615-658.

Morgenstern, N.R. (1991) Limitations of stability analysis geotechnical practice. Geotecnia, 61:5-19.

Munson, C.G. & Thurber, C.H. (1997) Analysis of the attenuation of strong ground motion on the Island of Hawaii. Bull. Seism. Soc. Am., 87:945-960.

Nadim, F. (2007) Tools and strategies for dealing with uncertainty in Geotechnics. Griffiths, D.V. & Fenton, G.A. (eds) Probabilistic Methods in Geotechnical Engineering, Springer, New York, pp. 71-96.

Navarro, J.M. (1974) Estructura geológica de la isla de Tenerife y su influencia sobre la hidrogeología. Actas del I Congreso Internacional sobre Hidrología en Islas Volcánicas, Lanzarote, v. 1, pp. 37-57.

NCSE-94 (1994) Norma de Construcción Sismorresistente: Parte General y Edificación, Real Decreto 2543/1994 de 29 de Diciembre, Boletín Oficial del Estado núm. 33 de 8 de Febrero de 1995, Madrid, pp. 3935-3980.

NCSE-02 (2002) Norma de Construcción Sismorresistente Parte General y Edificacón, Real Decreto 997/2002 de 27 de septiembre, Boletín Oficial del Estado núm. 244 del viernes 11 de octubre de 2002, Madrid, pp. 35898-35967.

Obermeier, S.F.; Pond, E.C. & Olson, S.C. (2001) Paleoliquefaction studies in continental settings: geological and geotechnical features in interpretations and back-analysis. U.S. Geol. Survey. Openfile Report, 01-29, 75 pp.

Obermeier, S.F. (1996) Use of liquefaction induced features for paleoseismic analysis. Eng. Geol., 44:1-76.

Ordaz, M.; Aguilar, A. & Arboleda, J. (1999) Program for Computing Seismic Risk. Instituto de Ingeniería, Universidad Nacional Autónoma de México, México City.

Pérez Torrado, F.; Paris, R.; Cabrera, M.C.; Carracedo, J.C.; Schneider, J.L.; Wassmer, P.; Guillou, H. & Gimeno, D. (2002) Depósitos de tsunami en el valle de Agaete, Gran Canaria (Islas Canarias). Geogaceta 32:75-78.

Seisdedos, J. (2008) Large Paleo-Rokslides of Güimar and La Orotava (Tenerife): Geological Analysis, Instability Mechanisms and Geomechanical Modeling. PhD Thesis, Universidad Complutense de Madrid. E-prints Complutense, Madrid, 512 p.

Simpson, D.W. (1986) Triggered earthquakes. Ann. Rev. Earth Planet. Sci., 14:21-42.

Smith, K. (2001) Environmental Hazards. Assessing Risk and Reducing Disaster. 3rd ed. Routledge, London, 392 pp.

Varnes, D.J. (1984) Landslide Hazard Zonation: A Review of Principles and Practice. UNESCO, Paris, 64 pp.

Ward, S.N. & Day, S. (2001) Cumbre Vieja volcano potential collapse and tsunami at La Palma, Canary Islands. Geophys. Res. Lett., 28(17):3397-3400.

Wells, D.L. & Coppersmith, K.J. (1994) New empirical relationships among magnitude, rupture length, rupture area, and surface displacement. B. Seismol. Soc. Am., 84:974-1002.

Whitmam, R.V. (1984) Evaluating calculated risk in geotechnical engineering. Proceed. Geotech. Div. Jl. of the American Soc. of Civil Engineers, 110(2):143-188.